Response to the reviews of the manuscript "Analysis of the Surface Mass Balance for Deglacial Climate Simulations" submitted to The Cryosphere.

We thank both reviewers for their comprehensive reviews and very useful suggestions to improve the manuscript. We have addressed all of their comments and believe that the changes will significantly improve the manuscript. In the following, reviewer comments are highlighted in blue, author responses in black.

Anonymous Referee #1

General comments

I did enjoy reading this, and it feels like I've spent a lot of time writing it up – apologies for the lateness - I found lots of small things to ask about, see below.

We thank the reviewer for his very comprehensive review and are glad for the very good suggestions to improve the motivation and framing of the manuscript.

I felt there was one wider, general issue that hopefully would be easy enough to address - as I got to the paleoclimate section I didn't think that a solid motivation had really been given for /why/ a simulation of deglacial SMB was being done, and thus I wasn't really sure what to be looking for in how it's been described and analysed. Even by the end this isn't clear, as the Conclusions don't conclude anything that sounds obviously new about the glacial climate system or the model itself. In a couple of places it's said that the SMB fields will be made available to the ice sheet community for their use, but the first part of section 4 says that the simulation isn't going be evaluated, so I don't really buy this as sufficient motivation for the whole exercise - are these modelling groups going to want to use a new SMB product from a climate simulation that hasn't been evaluated for how it compares to evidence of what actually happened?

We agree that the motivation of this analysis did not come out clearly in the manuscript. We changed the abstract and introduction to state our motivation more clearly. The main motivation for our study is that for long term studies of ice sheet changes (fully coupled climate-ice sheet or ice sheets model only simulations) realistic SMBs derived from long Earth System Model (ESM) simulations are needed. Here, we present an EBM that is used to downscale coarse resolution ESM output. We evaluate the EBM and apply it to the first transient simulations of the last deglaciation with the MPI-ESM earth system model and prescribed ice sheets. A misunderstanding is that these simulations are not evaluated. We are currently undertaking an analysis regarding the sensitivity of the experiments to differences in the boundary forcing (Glac1D vs Ice6G). A publication of the results is expected in the near future.

There is some interesting decomposition of how accumulation and melt factors balance differently in different periods and how the (perhaps non-obvious) relationship between total SMB and ELA changes too, but only for GrIS - is it different in different regions? - and no attempt is made at general statements about the global implications or testable hypotheses for underlying principles. Personally, I wanted to know more about how some of the details of the snow physics were being forced by the climate through the deglaciation - albedo, refreezing etc, rather than just the resulting SMB, but that's just one idea.

We shortly discuss these changes in the section for the Laurentide and Fennoscandian ice sheets. However, there are different processes acting across these ice sheets as they respond to both changes in the Atlantic and Pacific. So the relationships are not uniform over the ice sheets. We believe that part of this comment is also related to the confusion of the melt definition (see comment to line 252) - we now defined the melt explicitly in the manuscript, which includes refreezing processes. We also revised the introduction and specifically the motivation for this study, which is to simulate a realistic SMB for long-term studies of ice sheet and climate interactions. Thereby, we hope to have addressed the concerns of the reviewer.

I think the authors should either decide on a clear main goal that's stated at the front of the paper and runs all the way through, or be more clear about the separate aims of each part - either way that should make it easier to see what the paper as a whole is working towards, and clearer what should be in the final conclusions.
We revised the introduction and parts of the conclusion to emphasize our motivation and the aim of the present paper.

Detailed comments:
line 4: "deglacial climate" - quite specifically the /last/ deglaciation
We changed it to 'the last deglaciation'

line 5: "allows to resolve" isn't grammatically great - 'allows the resolution of' perhaps?
Thanks, we changed this.

line 8: The flow of ideas implied by the: 1) <multiple sentences> 2) structure isn't very clear, I'm not sure it's needed
We removed this and rephrase slightly.

line 10 (and throughout): I found the dating notation used throughout off-putting, personally, but that might just be me. In my experience, the convention I've seen most is that kyr = "thousand years" and ka = "thousand years ago" with 1950 usually taken as the reference for 'ago'. "ka BP" thus feels to me like it's mixing conventions and providing both an 'ago' and a 'before'. I could live with the use of "ka BP" if defined here carefully (and used consistently throughout, but sometimes just "ka" seems to be used to indicate an event date, not a period of time - I'm looking at line 447 as I type this, and table 2 has "kas BP"), but I'm afraid the use of just "a" as the shorthand unit for years (and is that actually meant as 'years before 1950'?), spaced away from the number it's attached to so it can be mistaken for the indefinite article 'a', just grated horribly for me - eg line 455, line 359. It looks OK for eg the SMB numbers as (Gt aˆ-1) - to avoid confusion perhaps write the full word 'years' in cases like line 359 where "a" is currently used on its own? Related to the date convention, the only place I saw the 1950 reference date stated for the BP 'present' is in the caption to figure 3, and since this isn't a paleoclimate-specific journal I think it would be helpful for the readership to note this much earlier and more plainly.
Thank you very much for the clarification. We revised the manuscript in respect to the notation mentioned here and introduce the reference year (1950) earlier in the manuscript.

line 11: having said that melt dominates the changes at 13ka, it would be helpful to say which component causes the increase in SMB at 9ka - is it an increase in melt or decrease in accumulation?
We added 'After 13 ka the increase in melt begins to dominate the SMB decrease'.

line 12: would be helpful to note the timescale of this AMOC/SMB variability here, it it related to eg Heinrich events or slower/different variations
We will add 'centennial-scale episodes'.

line 13: not sure a statement on data availability needs to be part of the abstract does it, that intent is implicit in EGU journals now?
It is not and we removed it from the abstract. Thanks for the suggestion.

line 25: a lack of local horizontal resolution is far from the only reason ESMs struggle with ice sheet SMB - large-scale background climate and circulation biases play a big role, and increasing resolution (horizontal and vertical) certainly doesn't solve everything for either Greenland or Antarctic surface simulations in global models.

We do agree with this point and mention these shortcomings by including *"This is specifically challenging, as ESMs exhibit biases and the horizontal resolution is often not sufficient to capture small scale climate features, e.g., sharp topographic gradients at the ice sheet margins as well as cloud, snow and firn processes (e.g. Lenaerts et al. 17, van Kampenhout et al 2017, Fyke et al. 2018)."*

line 28: this paragraph is still supposed to be about ice sheets generally, but all these references are for Greenland SMB. You could throw in some Antarctic studies too to be a bit more general - eg Agosta et al., TC 2019

We added some references about SMB changes over Antarctica (Lenaerts et al., 2012b, van Wessem et al., 2018).

line 29: I spent a while wondering which ice sheets were going to be included in this study, and it's not clarified until much later in the paper. This would be a good opportunity to say this - 'extends the analysis of northern hemisphere SMB changes', perhaps? - and also a good place to note why it's of interest to have a detailed SMB product / analysis for this domain.

Thank you for your suggestion! We included that we are analyzing the northern hemisphere. And we add a short paragraph why we need realistic SMBs specifically for this region and time period. We added in the end of the paragraph: *"These climate changes and the variability associated with the changes in the northern hemispheric ice sheets during the deglaciation and the resemblance to the expected future climate change emphasize the need for a realistic representation of the SMB for past and future stand-alone ice-sheet and coupled climate-ice-sheet model simulations (Fyke et al., 2018)."*

line 37: references for what different proxy studies suggest about AMOC variation during these periods would be useful

We added some references (Heinrich 1988, Keigwin et al 1994, Vidal et al 1997).

line 45: I think this statement is too strong - Bauer and Ganopolski show that using fixed parameter values throughout in their simple PDD model does a poor job, but inverting that to say that *only* EBM models can produce realistic ice volume changes seems too much. I'm a little wary as well of the way the term "EBM" might be taken by readers too, whilst we're on the subject - in my (climate modeller) experience it's most often used in the sense of a much-simplified model of radiation balance for an atmospheric column, but here (I think) its being used in a much more general way for any model that explicitly calculates the components of the energy budget and how they affect temperature and the phase of water at the surface, however complex or simplified. This potential confusion could be eliminated by a disambiguation sentence?

We use the term EBM more specifically as synonym for a model that is used to calculate and downscale the surface mass balance from ESMs independent of its complexity. We are excluding PDD models, which use statistical relationships between melt and temperature patters based on present-day observations. We changed the sentence in response to this review and reformulated the motivation for this study.

line 53: typos: "a EBM" and "Two kind of simulations"

Thanks for pointing these out!

line 62: this is OK for present-day Greenland (although the accumulation isn't a simple function of height), but should this relationship be taken to be equally strong for all ice sheets, all the time? For example, variation in present-day Antarctica SMB components is more significantly controlled by dynamic atmospheric conditions, rather than a local scaling with topographic height I'd say. Might be worth a caveat here, and a sentence in the discussion about the limitations of this sort of downscaling

We added a note in the paragraph that emphasizes that the elevation dependence is not all there is: *“Note, that an elevation dependence of the SMB components is a simplified assumption and valid mainly for present-day Greenland. Atmospheric dynamics also significantly contribute to variations in the SMB components, specifically over present-day Antarctica.”*

line 78: can the intervals/level heights be detailed in a table, maybe supplementary material?
We added a Table to the supplementary material.

line 84: it would be helpful to note in this list that the phase of precipitation may be changed too
We added: *“Total precipitation rates (liquid and solid) are corrected under consideration of the height-desertification effect. This halves the precipitation for an orography height difference of 1000 m above a threshold height of 2000 m for each grid point (Budd and Smith, 1979). Note, that snowfall is determined from the total precipitation for height corrected near-surface air temperatures below 0C within the EBM.”*

line 105: does the rain that potentially refreezes have a temperature, - perhaps that of the surface - changing the amount of energy required to refreeze it?
We added *“The temperature of rain is assumed to be equal to the height corrected near-surface air temperature.”* for clarity.

line 141: I found it confusing to say "the aging process starts", when so far the only aging process described is for fresh snow. ’Another aging process starts’, perhaps? Your aging of the surface albedos is purely a function of time, when quite often the rate of increase of snow-grain size and thus lowering albedo is dependent on temperature and density. Do you know how sensitive your results are to the timescales you’ve chosen, and whether you would expect them or your results to be different for LGM temperature and accumulation rates?
Here, it is not another aging process but the aging of the albedos as described above. Maybe ‘the aging process starts from the beginning’ would clarify? The parametrization used here goes back to Oerlemans and Knap (1998). We did not do a comprehensive testing regarding the sensitivity to the length scales, as we mainly followed the parametrization in the above mentioned reference. Also computational limitations for the long-term simulations make several attempts with different tuning factors not feasible.

line 155: Going on with the thread of the previous comment, any table of tuned values almost begs the question of how sensitive your model is, and conclusions are, to the choices you have made, especially when they have been tuned to match one type of climate (the present GrIS) and the model is then applied to very different ones. Do you have any insight from your undocumented(?) tuning process that you could use to comment on this sensitivity? More work, but maybe possible if you have already done (or could easily do?) the simulations, would be to not only compare your results with MAR SMB for the present, but also for what other models find for GrIS SMB at 2100, or under some other idealised climate forcing. Freely downloadable results do exist for MAR run to 2100 with the climates from various CMIP6 models, from the ISMIP6 preparations. That wouldn’t be an evaluation in the same way, but would give your readers some useful reference points for how sensitive your EBM tuning is to the climate it’s in.
The SMB derived here is sensitive to all of these tuning factors, which is the reason why we chose to present the values in the Table. As for any tunable variable in a model we made the choice between being as close as possible to present-day observations and model performance. Due to computational limitations for the long-term simulations we have chosen one set of parameter for the deglacial simulations, hence, we do not know how sensitive the

choice is under a changing climate. That being said, we are not confident that a comparison of the SMBs in a future climate with MAR will allow us to fully evaluate the obtained SMBs for a changing climate. It will be difficult to disentangle the effects on the SMB that arise from differences in the climate forcing itself (MPI-ESM vs. MAR forcing). However, we applied the EBM to a simulation with the MPI-ESM high resolution setup for the SMBMIP inter-comparison and the results showed that the setup was specifically good in representing the trends of the Greenland mass loss between 2003-2012, indicating that not just the SMB mean climate over Greenland, but also changes in the climate are represented reasonably well as compared to observations and RCMs (see Fettweis et al., 2020). We added the following information to the manuscript: *"The same parameters were applied in an EBM simulation forced with output from a high resolution MPI-ESM simulation for historical climate conditions within the scope of a SMB model inter-comparison (SMBMIP; Fettweis et al. 2020). The results showed that the derived SMBs were very similar to observations in terms of the SMB mean climate as well as the SMB trend (2003-2012)."*

line 161: I had trouble following this section, but I think I more or less got there in the end. Might be worth thinking about rephrasing. The two cases handled are labelled 1) and 2), but that numbering isn't used again, and it seems like the first case described ("The inflow of snow and ice from above") is actually case 2). How does the temperature profile shift - in proportion to the amount of mass (solid and liquid?) that has been moved between layers? In the case of surface melting (line 165), the mass has not actually left the snowpack until the percolation/refreezing procedure has been completed, so is the change in density profile delayed until that has been done? Although,surface melting lifts the profile /up/, which sounds like melting at the surface makes the top layer /more/ dense than the reference. How does the surface layer ever reduce again to the reference profile, since more snow falling should further increase the layer density (line 163) or be directed to other layers underneath? Is it said anywhere what the top/bottom densities in this profile, or the density of ice in the virtual under-layer, are?
We have revised the complete paragraph for clarification under consideration of the questions mentioned here. The procedure applied here is instantaneous. We first calculate compaction and then surface melt. Percolation and refreezing can affect the density profile. The temperature profile follows the movement of mass. We also tried to clarify how the density profile changes for different conditions. The top and bottom densities are those of ice and snow. We hope that the rewritten section allows for a better understanding of the used parametrization.

line 190: is even the deep ocean in a true steady state for your LGM initial condition, or are there drifts there to worry about? If it's all a steady state, why are first 5 kyr considered a discardable spin up?
Note that these are transient simulations of the last deglacation, hence, there is no steady-state. We initialized the simulation from a spun-up glacial steady-state at 26 ka. We are only investigating the last 21 kyrs for the model to adjust to the changes and because this is the most interesting time period. 5000 years are enough to capture the drift in the deep ocean. Therefore, we considered the rest as additional spin-up. As this seems to confusing we rephrased.

line 195: Freshwater input forced AMOC variability comes up as a feature later - it would be good to mention specifically how glacial runoff/outburst water is treated in their protocol
We added following information: *"Freshwater from melting ice sheets is calculated from the volume changes in the ice sheet reconstructions for each grid point. For grid cells over land melt water is distributed through the hydrological discharge model, over ocean it is discharged into the adjacent ocean grid cells. "*

line 200: From figure 4 etc, it seems like the ELAs talked about here are not a simple contour on the ice surface demarking where ablation and accumulation balance, but a /potential/ ELA calculatable for the climate in each land surface gridbox regardless of what the actual altitude (or SMB) of the ice sheet was. I'm still not sure what I think that means - precipitation, for instance, is at least partly orographically controlled and either falls in one place or another so it does matter where the surface really is, so not every potential ELA calculated can simultaneously be true...maybe?...but anyway, it would be worth another sentence to explain that the ELA that will be talked about from here on is not a simple contour line on the ice.
We included a sentence that clarifies the ELA used in this study, which is indeed a potential ELA, as it is calculated in each grid point. *"At heights above the ELA it is thermodynamically possible to accumulate snow throughout the year and form an ice sheet or glacier. At elevations below the ELA melt dominates accumulation and no ice sheet can form. Here, the ELA is calculated in each grid point, hence, resembles a potential ELA. It is a proxy for climate changes affecting the ice sheets. "*

line 202: since the ELA is defined as the height where SMB=0 I don't really see what is meant by saying it's less sensitive than SMB
To obtain realistic SMBs we need to downscale the SMB onto a different grid (to the ice sheet topography from the reconstructions), while the ELA can be determined directly on the atmospheric model grid. The downscaled SMB shows enhanced melt patterns specifically at the margins of the ice sheet where the simulated climate from the coarse resolution model and the high resolution ice sheet topography potentially do not fit together (in a fully coupled simulation an ice sheet would likely not survive in these areas). If these values are integrated, the resulting SMB may be underestimated. Integrating the ELA on the native model grid allows for a more model consistent representation of patterns. Hence, it is less sensitive than the SMB. We rephrased this sentence to make it more clear. *"As the ELA estimate is calculated on the native model grid it is more consistent with the model physics and boundary conditions used in the simulations than the downscaled SMB. Hence, integrated values of the ELA are less sensitive to changes in the ice sheet mask than those of the SMB. "*

line 232, 242: structurally, do these short paragraphs need their own section headings? Thinking about it, would it make more sense to put the paleo experiment design section later, next to the paleo results, rather than right up front before all the recent history stuff is described and analysed?
These are good points but we have decided to put it this way around, as our historical simulations are branched off from the deglaciation experiment. So to describe the recent history simulations we believe we need to describe how we initialized them. To avoid too much repetition we therefore decided to put it this way around. We changed the sub headings to "Evaluation Data" to avoid too many subtitles and hope that this is sufficient.

line 238: not just cloud, all precipitation in ERA - and thus your EBM-ERAI GrIS accumulation - is also purely a product of their model physics run at global resolution, so I wouldn't expect that to make for a great comparison with the local MAR precipitation, regardless of how well EBM-ERAI can do the surface energy balance.
We fully agree with the reviewer. This sentence was meant for readers not fully aware of the limitations of reanalysis. We added some examples (precipitation, clouds).

line 252: from here on, neither refreeze nor runoff is mentioned, only "melt". Since we're often talking about total SMB, I'm not sure whether they really mean surface melt (that might refreeze), or the actual liquid mass leaving the snowpack (runoff). Or are they talking about runoff-precipitation - so the proportion of the original mass that has now been lost? I'm interested to see what their refreezing does anyway, and it's a shame that that's not

mentioned, but if they really are talking about just surface melt from here on then I really think the refreezing needs to be shown too.
We believe that we have introduced melt in the introduction *" The SMB is determined by mass gain due to accumulation, as a result of snow deposition, and mass loss by ablation, induced by thermodynamical processes at the surface and subsequent melt-water runoff (Ettema et al., 2009)".* Here the melt is defined as the mass leaving the snowpack, that means melt water that refreezes is not considered in this estimate. We added a sentence to clarify this definition. *"In the following, accumulation is defined as mass gain due to snow deposition and melt as mass loss due to ablation (often referred to as runoff). Refreezing processes are considered in the melt estimate."*

line 269 (and I elsewhere, like line 316): there's a tendency here to simply blame the biases on in the MPI-ESM runs and the EBM SMB derived from them on inadequate spatial resolution and the local topography. That will undoubtedly be part of it, especially at ice sheet margins, but higher resolution doesn't fix everything in complex climate models, in fact it can make it worse (see Kampenhout et al, TC, 2019 for a very geographically relevant case-study). Biases in the large-scale climate, inappropriate initialisation, internal variability, missing physics - the list is of course endless, so it's irksomely simplistic to keep saying that the model resolution is too low and no more. It's not like the EBM_MPI-ESM results would = EBM_ERAI if you just ran MPI-ESM at ERAI resolution.
We are aware that model resolution is not the only reason for the discrepancies between MAR, EBM_ERAI and MPI-ESM-LR and MPI-ESM-CR. In fact, there are many uncertainties in our system, related to biases in the model climate (clouds, precipitation, surface processes, ...), the parametrization used to downscale the SMB (including e.g. a constant lapse rate over the whole ice sheet) and of course the vertical and horizontal interpolations from the elevation classes on coarse resolution to the high resolution ice sheet topography. We revised the manuscript throughout and added specifically *"The comparison between EBM_MPI-ESM-LR and EBM_MPI-ESM-CR indicates that an increase in resolution cannot resolve all biases. This is in line with findings by Kampenhout et al. (2019), showing that a regional grid refinement in simulations with the Community Earth System Model (CESM) did not improve all SMB components. Model biases, e.g. in the large-scale circulation, clouds and precipitation patterns (Mauritsen et al., 2019), as well as uncertainties due to internal variability are exhibited in all ESMs and explain part of the differences seen in the presented comparison."* and also revised other places throughout the manuscript (e.g. line 316). We also believe that we have discussed other possibilities in the discussion section: "*A comparison with SMBs derived from a simulation with the MPI-ESM-LR setup and ERA-Interim reanalysis reveal that discrepancies between the SMBs derived from MPI-ESM-CR and MAR are a result of the coarse resolution of the model (e.g., the extensive melt in the North of the Greenland ice sheet) and due to the quality of the forcing itself (e.g., precipitation patterns). In contrast to ERA-Interim, MPI-ESM evolves freely and does not assimilate any surface observations; hence, differences are to be expected. Further differences are related to underlying topographies of the native models as well as the fact that most fluxes within the EBM are parameterized, as they are not directly available from the model simulations in the required temporal resolution."*

line 275: RACMO hasn't been introduced yet in any way, as a model or an acronym
Thanks, we introduced the acronym here.

line 276: You have some tunable control over the rain/snow partitioning in your EBM, so could this MPI-ESM bias be fixed for your purposes?
Precipitation is considered as snow if the height corrected near-surface temperatures are below 0C. This would be of course a tunable value, but we do not believe that it is very physical to change this relationship.

line 281: I would have thought that larger-scale moisture transports over the ice sheet,

which are also quite resolution dependent, would be likely to play a role here too. Low resolution atmospheres often just drizzle too far north and over too-wide areas because they're overly diffusive everywhere, it's not just a local thing you would fix with a higher ice sheet. Again, maybe this is an area where things in the climate models other than simply local grid resolution/topography play a significant role
This is likely also a contribution but we believe it is rather remarkable how differences in the topography match the differences in the precipitation. This points to the topography being the dominant driver of those difference, but does not rule out other processes. As we added a couple of sentences in response to comment line 269 we believe we have covered this point.

line 295, 300: I didn't follow the logical thread through here. First MPI-ESM-CR has a higher topography than MAR and the EBM produces too much melt, then later the area in the south is higher than the ISMIP topography and there is less melt. Less melt in which model? Is there a consistent physical link being drawn between these two cases?
We apologize for the confusion. The first sentence should read *"has a higher topography than ISMIP..."* - as is shown in Fig. 2. We believe that we explained the physical mechanisms by *"One problem of downscaling melt in these regions is that temperatures are always at the melting point during melting. By projecting the temperatures onto lower elevations, the height corrected temperatures depart significantly from the melting point towards higher temperatures. Hence, the vertical downscaling from higher elevations to low elevations overestimates melting"* and that the reason for the confusion lies in the small error.

line 299: your model has a pretty direct control on how much melting you get when you adjust for a new elevation through the lapse rates - does this point to the lapse rate changes being too high?
This is a good question. The lapse rate is used in the model as tuning parameter and we have chosen a value that results in realistic SMBs for the whole Greenland ice sheet. In the current version of the model it is considered as relatively low (4.6K/km), which certainly is at the lower end for Greenland temperatures. It points towards the challenges in using one constant lapse rate over all ice sheets and certainly is a shortcoming in our EBM.

line 323: I think this statement on the scope of the paper should be in the Introduction, not all the way back here
We moved this sentence up in the introduction. Thanks for the suggestion.

line 329: The Antarctic ice sheet has yet to collapse, thankfully
We fully agree and added 'all northern hemispheric ice sheets'.

line 332: It would be good to say why these particular time-slices are chosen for analysis.
These time slices show the most significant changes during the deglaciation. We added this information. "... in order to indicate the most drastic changes in the northern hemispheric ice sheet configuration."

line 344, 396: the impact of the changes in circulation and the different realisations of AMOC history on the ice sheet SMB sound interesting, it would have been good to hear more about them and how that might have influenced the ice sheet deglaciation. There is some decomposition of whether accumulation or melt is dominating the SMB/ELA trend for the main Glac1D run at different periods - does all this still hold for the ICE6G run? If so, that's an interesting conclusion perhaps that you can say is independent of the ice sheet reconstruction used.
Good point! We added some information on the atmospheric circulation changes (see also comments by reviewer #2). We also see similar melt-accumulation relationship for the Ice6G simulation, although the absolute magnitude differs. Melt is close to zero until about 14 ka

and also reduces during the major AMOC slowdowns. Note, that the AMOC slowdowns are somewhat different in their timings and occurrence, due to uncertainties in the reconstructions - something we are currently investigating in a separate study. As the relationships hold we included a sentence pointing this out. Thanks for this suggestion.

line 394: the final figure of 550 Gt/a doesn't match the values in your table /very/ well. Does the 550 at the end of the transient correspond to the year 1950, rather than _2000? Your recent history run does go through 1950 doesn't it, even if only 1980-2010 were analysed - does this 550 match what the historical run did at that point?
The historical simulation is somewhat different from the transient simulation, as it includes more realistic forcings (e.g. volcanoes, land use, anthropogenic forcings). Therefore the SMB values at the end of the transient simulation (1950) are higher than in the beginning of the historical simulations. The differences in the forcing are also the reason why we performed the last millenniums simulation (starting at 1850 from the deglaciation experiment), in order for the model to adapt to the changes in the forcings. Hence, we have no overlap between the end of the deglaciation and the historical simulation to directly compare the values. We revised the sentence to *"These values are similar to values observed during the 21st-century, although slightly higher as no anthropogenic forcings are considered in the deglaciation simulation (see Fig. 4, Section 3 and Table 3)"* for clarification.

line 403-405: references needed for the decline history of these glacial ice sheets
We added references to this section.

line 450: this information about the meltwater forcing should be in the experiment description
As we included how we determine the freshwater flux from the ice sheet reconstructions in the experiment section in response to an earlier comment we believe that this is covered. The melt water pulse is prescribed by the reconstructions, which are introduced in the experimental description.

figure 1: is this surface melt, or runoff: the caption says ACC = SMB - MELT? It also says that MAR does not provide accumulation, which I don't understand - MAR gives you snowfall and rainfall? The ELA is just the contour of where the SMB on the surface is 0, isn't it? Is it said in the text why CR has so much more melt in far north
Accumulation in our study is defined as the mass gain due to snowfall. While MAR provides snowfall and rainfall it does not explicitly provide how much of the precipitation accumulates over the ice sheet. We believe that calculating it as residual is therefore the right thing to do. We believe that melt in the north of the ice sheet is a result of the underlying topography (and to some extent probably also model biases) and cite from the text: *"Comparisons with EBM_MPI-ESM-LR, which shows less melt in the north and west of the ice sheet as compared to EBM_MPI-ESM-CR (Fig. 1 and 2), confirm that differences in the melt patterns are linked to the underlying topographies of the model versions. MPI-ESM-LR is slightly higher than MPI-ESM-CR and thereby closer to MAR on the northern and western flanks of the ice sheet, hence EBM_MPI-ESM-LR$ shows less melt than EBM_MPI-ESM-CR in these areas."*

fig 2: (top, middle) to denote the second row and (bottom, middle) to denote the third row is not very clear. Ditto (center, left) and (center, right). With this many panels may just label them a)-p)?
We added labels to Fig. 1 and Fig. 2. Thanks for the suggestion.

fig 3: Paleoclimate figures often stack different proxies on the same horizontal time axis but offsetting the vertical axes, rather than overlaying everything completely like this - that might work well here too.

Thanks for the suggestions. We are aware of these plots but think that in the current presentation relationships between e.g. the ELA and CO2 as well as the MOC are easier to see and interpret. Similarly for melt and accumulation relationships.

fig 4: the 2D ELA surface idea might need explaining in the caption here too. Is the EBM run everywhere? Is there +SMB in the MPI-ESM climates for other places, eg a Siberian ice cap that's just not shown here because masking teh results onto the Glac1D glacier mask?

We clarified the ELA definition and that we masked the SMB and ELA with the glacier mask by including "*The SMB is interpolated on the Glac1D topography for each individual time slice and masked with the Glac1D glacier mask. The ELA, defined as elevation where the SMB equals zero, is calculated for each grid point on the native MPI-ESM-CR model grid from the 3-D SMB in each grid point (see Sections 2.1 and 2.3). The ELA is masked with the glacier mask used in the MPI-ESM-CR simulations.*"

Anonymous Referee #2

Major comments:

My only slightly larger comment has to do with a lack of discussion and references of literature on atmospheric circulation changes at the LGM and through the deglaciation. You mention several times that the atmospheric circulation changes over this time period, but no previous studies are cited. Atmospheric circulation changes is arguably not a main focus of your study, but it is a nice gesture to acknowledge work that has been done on this topic in the last several years, not least since it is relevant for your overall modeling approach and for the interpretation of your results. It is generally accepted that the North Atlantic jet stream and storm track was quite different at the LGM than it is today. Specifically, modeling simulations suggest that the large scale circulation was more zonally oriented than today. Several explanations for this has been proposed, but the most recent explanation (that links all previous interpretations into one theory of the zonal North Atlantic jet stream and stormtrack is described in:

https://www.sciencedirect.com/science/article/abs/pii/S0012821X20300248

A recent overview paper on the PMIP4 LGM simulations:

https://cp.copernicus.org/preprints/cp-2019-169/

Circulation changes in the North Atlantic and over Greenland over the last deglaciation: https://agupubs.onlinelibrary.wiley.com/doi/full/10.1002/2017GL074274

https://agupubs.onlinelibrary.wiley.com/doi/full/10.1002/2015GL066042

https://cp.copernicus.org/articles/15/1621/2019/

We fully agree with the reviewer and thank him for referring to the literature. The atmospheric circulations plays an important role in our simulations and we find similar changes in the atmospheric circulation during the LGM, as described in Löfverström and Lora (2017). In a study currently under preparation for publication, we also find that uncertainties in the ice sheet reconstructions lead to significant differences in the atmospheric circulation. As we focus on the SMB and drivers of SMB changes in the current manuscript, we will mainly touch on these processes in the revised manuscript (see detailed response below).

+++++++++++++++++++++++++

Line comments:

Page 1, line 3: comprehensive -> high complexity?

We change to state-of-the-art as we believe that these models are both comprehensive (in their sub-model components) and have a high complexity.

Page 1, line 5: "downscale atmospheric processes" I assume that you mean radiation?

In this case we downscale the energy balance at the surface, more specifically the SMB, accumulation and melt, not just radiation. We changed the sentences to *"An energy balance* *model (EBM) is used to calculate and downscale the SMB on higher spatial resolution and allows the resolution of SMB variations due to topographic gradients not resolved by the ESM"* for clarity.

Page 1, line 6: Here and elsewhere. Maybe more appropriate to say "satellite era" or "recent past" instead of historical period. The latter is used to describe 1850 – present in CMIP6.
This is correct, but they are also labeled as historical in the CMIP experiments. We believe that defining the years of our analysis and introducing the period as historical is sufficient here.

Page 1, line 7: "from regional modeling" — add that this is constrained by reanalysis data at the lateral boundaries
We did not add this in the abstract, but into the introduction, as it is an important information that we did not mention throughout the manuscript. Thanks for the suggestion.

Page 1, line 10: Specify that you refer to Northern Hemisphere summer insolation
Thanks for pointing this out. We changed this.

Page 1, line 19: Here is a relatively recent, comprehensive review that may be worth mentioning in this context: https://agupubs.onlinelibrary.wiley.com/doi/full/10.1029/2018RG000600
Thanks for pointing us to this review. We added the reference to this review in the beginning of this section in response to another comment.

Page 2, line 35-36: Good place to mention some work on atmospheric circulation changes in the last deglacial period
Thanks. As mentioned before we extended this paragraph and included some information on circulation and climate changes as well as some of the proposed references: *"The collapse of the ice sheets also resulted in significant changes in the atmospheric and oceanic circulation as well as associated climate features (e.g. Lofverstrom et al. 2017). Orographic changes, induced by the decrease of the Laurentide and Cordilleran ice sheets, led to changes in the Northern Hemispheric stationary waves and thereby the North Atlantic jet stream, which significantly affected the northern hemispheric climate (e.g. changes in precipitation and temperature patterns; Andres and Tarasov, 2019; Lofverstrom et al. 2020, Kageyama et al. 2020)."*

Page 2, line 36: "Atlantic Meridional Overturning Circulation"
Thanks. We will change this.

Page 2, line 42: "Mainly" is repeated. Maybe change the latter to "employed"?
Thanks! Changed.

Page 3, line 53: Two kind -> Two kinds
Thanks. Changed.

Page 3, line 54: Again, not sure if "historical" is the best word here
Please see comment above.

Page 3, line 56: SMBs to SMBs — awkward wording
We rephrased to *"...compare obtained SMBs to output from the regional climate model MAR".*

Page 3, line 60: Meaning here is not clear. How do you use an EBM to downscale SMB? Do you mean that the radiation from the EBM is downscaled, or something

else?
We rephrased the sentence to *"We use an EBM to calculate and downscale"*... Surface fields from the MPI-ESM simulation are used to calculate the SMB, which is then interpolated on a higher resolution ice sheet topography. Note that we not just correct radiation but also precipitation, pressure, etc.

Page 3, line 60: What influence of clouds? SW radiation? LW radiation?
We are not sure what is meant here, as clouds are not mentioned in this sentence. We assume that the reviewer is talking about Line 69, where we can add *"The main improvements are 1) an advanced broadband albedo scheme considering aging, snow depth dependency, and the influence of the cloud coverage on the thermal radiation,..."*

Page 3, line 70: Meaning of "movement of the snow/ice properties and compaction" is not clear
We rephrased to "the consideration of snow compaction and the vertical advection of snow/ice properties".

Page 3, line 71: Explain what elevation classes are
Page 3, line 72: It was technically Lipscomb et al, 2013 that introduced elevation classes in the model https://journals.ametsoc.org/jcli/article/26/19/7352/34179/Implementation-and-Initial-Evaluation-of-the
We addressed both comments by changing: *"We further adopted the scheme by introducing elevation classes, following Lipscomp et al. (2013). Calculating the SMB on fixed elevation classes, has the advantage that the model becomes computationally cheaper, as the SMB is computed on the native and coarse resolution atmospheric grid instead of the high-resolution ice sheet topography."*

Page 3, line 80: How is the lapse rate for these factors determined? Also, do you use the same lapse rate in summer and in winter? If yes, is this a valid assumption? What is the sensitivity to this choice?
The lapse rate for the corrections is constant over time and space, which is a caveat in our method. As we are using a global model it is challenging to incorporate different lapse rates for summer and winter, as it would require lapse rate values that depend on the location (e.g. southern and northern hemisphere). As we have a very different ice sheet configuration during the LGM as compared to present day we would not like to make variables location dependent. Also, it is not certain how these values would change for different climates and over different ice sheets. Here, we use values based on present-day estimates with a bias towards summer values (see also comment to Page 4, line 87).

Page 4, line 85: Not sure if I understand this description. How do you conserve water if this is the case?
Note, that we only use the MPI-ESM output as forcing for the EBM. Hence, we do not need to conserve water and it is irrelevant here. In a fully coupled simulation, where interactive ice sheets are included, this would lead to discrepancies but can be corrected through run-off.

Page 4, line 87: This lapse rate is quite a bit lower than the ICAO value of -6.5 K/km. Explain this choice, and did you test the sensitivity to this value?
The lapse rate is used in the model as tuning parameter and we have chosen a value that results in realistic SMBs for the present-day Greenland ice sheet. In the current version of the model it is considered as relatively low (4.6K/km), which certainly is at the lower end for Greenland temperatures. However, it has been shown that over ice sheets near-surface lapse rates are significantly lower than the ICAO values, specifically during summer (e.g. Gardener et al., 2007). As we only use one lapse rate for the entire year and over all ice sheets we have chosen a relatively low value that still lies within observational values.

Page 4, line 97: Technical detail but what happens to (latent and sensible) energy fluxes if the atmosphere model simulates liquid precipitation, but the height corrected temperature is below freezing (and vice versa)?
The energy fluxes are calculated from the height corrected variables, so this should not be an issue here. We added *"Latent and sensible heat fluxes are parameterized and calculated from the height-corrected variables."*

Page 5, line 136: It is a bit clunky to define WE at the end of the sentence. Can this definition be moved earlier in the sentence?
Thanks for pointing this out. We moved this part of the sentence further up.

Page 5, line 141: brighten -> increase (?)
Thanks, we changed this.

Page 6, line 165: "Once: : :" — Meaning here is not clear. Do you mean that it is removed?
We rephrased the entire paragraph for clarity according to the comments of reviewer #1.

Page 6, line 180: Technical detail, but please specify that this is the horizontal resolution
Changed.

Page 7, line 189: Acronym "ka BP" is not defined
According to the comments of the first reviewer we changed all the year definitions throughout the entire manuscript.

Page 7, line 195: Not sure if I fully understand this modeling strategy. Do you run 10 years with a constant forcing before updating the boundary conditions, or do you advance the orbital clock, topography, etc. by 10 years every model year?
The first! In our setup the model is run synchronous in time but the forcing fields are updated only every 10 years. We changed 'updated' to 'prescribed' to clarify.

Page 7, line 196: What happens to vegetation in areas that are deglaciated?
We added a sentence to explain this: "*Land cells that are deglaciated are covered with the same vegetation form as the adjacent grid cells.*"

Page 7, line 203: "it is a good proxy" –> "hence, it is a proxy for..."
We changed this.

Page 8, line 214: " for a long enough adjustment" is a bit colloquial
We changed to 'sufficient'.

Page 8, line 232: Why did you use ERA-Interim instead of the newer ERA5? Do you expect different results with a newer reanalysis product?
We used ERA-Interim, as the regional models used for comparison here are all forced with ERA-Interim. Using the same background climate allows us to assess the uncertainties due to the downscaling techniques (regional modeling vs. EBM_ERAI). The derived SMB can only be as good as the forcing. As observations and assimilation over the Arctic regions are still sparse we do not expect a significantly better climate for another reanalysis product.

Page 9, line 250: : : :historical climate conditions -> recent past
See earlier comment.

Page 9, line 254: remind the reader that this is the "coarse" and "low resolution" simulations
We added a reminder.

Page 9, line 264: Say something about how these numbers change over Greenland

(latitudes of interest). Should be a factor of 2-3 difference from the equator
Thank you - it is a good idea to write the values for Greenland instead.

Page 10, line 286: Good reference https://tc.copernicus.org/articles/13/1547/2019/
Thanks for this reference. We added this reference and changed the paragraph according to the suggestions by reviewer #1.

Page 10, line 287: Sentence starting "The overestimation" is a bit clunky and can be simplified
Changed.

Page 11, line 316: What figure(s) are you discussion here?
We added a reference to Fig. 1 and 2.

Page 12, line 344: Good place to cite some work on atmospheric dynamics /circulation in the deglaciation. See major comment
Thanks, we did that! See comments above.

Page 12, line 354: shrinks -> recedes
Thanks! Changed.

Page 12, line 357: Further, it points towards the fact -> Further, it suggests
Thanks.

Page 13, line 380: typo: his -> its (?)
Yes.

Page 14, line 416: Even though the AMOC probably plays an important role for this response, it is the atmosphere that primarily interacts with the ice sheets. I would suggest extending this discussion with changes in the atmospheric circulation in mind, and perhaps cite a few papers that have looked at these interactions before
This is true, but we do believe that the AMOC changes are the trigger. Slowdowns of the AMOC lead to a significant cooling over the North Atlantic and the adjacent regions. Hence, they drive the changes in the surface temperatures that affect the SMB changes. All of this interaction is of course not possible without changes in the atmosphere. We tried to clarify this chain of processes and added references. We specifically added *"Another possible contributing factor to the pronounced SMB and ELA variability over the northern hemispheric ice sheets during this time period are changes in the atmospheric circulation. Lofverstrom et al. (2017) found that elevation changes of the North American ice sheet around the saddle collapse, defined by the separation of the Laurentide and Cordilleran ice sheets, caused significant changes in the stationary wave patterns. An amplifying factor for atmospheric circulation changes is the southward extension of the sea-ice cover due to the AMOC slowdown and reduced North Atlantic sea-surface temperatures. Such changes have a significant influence on downstream precipitation, evaporation and temperature patterns over the North Atlantic and adjacent areas." in the end of this paragraph.*

Page 15, line 467: What about regional and large scale atmospheric circulation?
We added feedbacks due to the ice sheet height, which includes atmospheric circulation changes.

Page 15, line 468: You could cite this paper when talking about other feedback processes: https://agupubs.onlinelibrary.wiley.com/doi/full/10.1029/2018RG000600
Thanks, we added this reference here.

Page 16, line 491: Can you end with a slightly more comprehensive future outlook?

Where do you want to take this in the future, and how will this new modeling capability be used in e.g. simulations of the future climate evolution, and/or other paleo-climate states?

We added some information of the future path of our research here: *“Utilizing the SMB data set presented here as forcing for ice sheet model simulations will allow for an investigation of ice sheet dynamics during the last deglaciation. In the future, we will utilize the EBM in simulations with an interactive ice sheet model, which is currently employed within the MPI-ESM setup in the scope of the project PalMod (Latif et al., 2016, Ziemen et al. 2019). This will allow to investigate feedback processes between ice sheets and the other climate components (see e.g. Fyke et al., 2018, for a recent review). It will also allow to investigate processes and test hypotheses arising from the deglaciation simulations for other climates, such as e.g. the last glacial inception, Marine Isotope Stage 3 as well as the future.“*

Table 2: This simulation contributed to CMIP6

Thanks. We changed this.

Figure 1: Here and elsewhere. Spectral colorbars are bad for people with color blindness. Please us a non-spectral color scale if possible

We have revised all figures and changed the colorbar.

Figure 4: Here and elsewhere. The SMB colorscale is a but crowded. If possible, use fewer intervals.

We have revised all figures and changed the labels, according the ones used in van Kampenhout et al., 2019.

Analysis of the Surface Mass Balance for Deglacial Climate Simulations

Marie-Luise Kapsch[1], Uwe Mikolajewicz[1], Florian Andreas Ziemen[1,*], Christian B. Rodehacke[2,3], and Clemens Schannwell[1]

[1]Max Planck Institute for Meteorology, Bundesstraße 53, 20146 Hamburg, Germany.
[2]Danish Meteorological Institute, Lyngbyvej 100, 2100 Copenhagen Ø, Denmark
[3]Alfred Wegener Institut, Helmholtz Centre for Polar and Marine Research, Am Handelshafen 12, 27570 Bremerhaven, Germany.
[*]now at Deutsches Klimarechenzentrum, Bundesstr. 45a, 20146 Hamburg, Germany.

Correspondence: Marie-Luise Kapsch (marie.kapsch@mpimet.mpg.de)

Abstract. ~~Most studies analyzing changes in~~ A realistic simulation of the surface mass balance (SMB) ~~of the Greenland ice sheet~~ is essential for simulating past and future ice-sheet changes. As most state-of-the-art Earth Systems Models (ESMs) are not capable of realistically representing processes determining the SMB, most studies of the SMB are limited to ~~the last century, due to the availability of observations and the computational limitations of regional climate modeling~~observations and regional climate models and cover the last century only. Using transient simulations with ~~a comprehensive Earth System Model (ESM~~ the Max Planck Institute ESM in combination with an energy balance model (EBM) we extend previous research and study changes in the SMB and equilibrium line altitude (ELA) for ~~deglacial climate conditions. An energy balance model (EBM)~~ the last deglaciation. The EBM is used to ~~downscale atmospheric processes. It determines~~ calculate and downscale the SMB on higher spatial resolution and allows ~~to resolve~~ the resolution of SMB variations due to topographic gradients not resolved by the ESM. An evaluation for historical climate conditions (1980–2010) shows that derived SMBs compare well with SMBs from regional modeling. Throughout the deglaciation changes in insolation dominate the Greenland SMB~~: 1)~~. The increase in insolation and associated warming early in the deglaciation result in an ELA and SMB increase. The SMB increase is caused by compensating effects of melt and accumulation, as a warmer atmosphere precipitates more. After 13 ka~~before present (BP)~~, the increase in melt begins to dominate and the SMB decreases. ~~2)~~ The decline in ~~insolation after 9 ka BP~~ northern Hemisphere summer insolation after 9 ka leads to an increasing SMB and decreasing ELA. Superimposed on these long-term changes are ~~episodes of significant~~ centennial-scale episodes of abrupt SMB/ELA decreases, related to slowdowns of the Atlantic Meridional Overturning Circulation (AMOC) that lead to cooling over most of the Northern Hemisphere. ~~To study associated changes in the ice sheet geometry, the SMB data set is made available to the ice sheet modeling community.~~

1 Introduction

Increasing contributions to sea-level rise from the Greenlandic and Antarctic ice sheets have led to an enhanced interest in processes that explain past and future ice sheet changes (see Fyke et al., 2018, for a recent review). Mass changes of ice sheets are controlled by variations in the surface mass balance (SMB) and ice discharge (van den Broeke et al., 2009; Khan et al., 2015). The SMB is determined by mass gain due to accumulation, as a result of snow deposition, and mass loss by ablation, induced by thermodynamical processes at the surface and subsequent melt-water runoff (Ettema et al., 2009). ~~Further,~~ Other processes resulting in mass changes of ice sheets are iceberg calving and basal melting at the ice-ocean and ice-bedrock interfaces~~impact the mass balance of ice sheets~~.

To model the SMB, atmospheric processes associated with the energy balance at the surface as well as snow processes, such as albedo evolution or refreezing, need to be simulated realistically (Vizcaíno, 2014). ~~This is specifically challenging~~ Therefore, most of the analyses on changes and variability of the SMB have been based on observations, statistical regression and correction techniques as well as simulations with high-resolution regional climate models (RCMs), which are constrained by reanalysis data at the lateral boundaries, and cover the last century only (e.g., Fettweis et al., 2008; Ettema et al., 2009; Hanna et al., 2011; I
. However, for long-term ~~climate simulations with~~ studies of past and future ice-sheet and climate changes output from state-of-the-art Earth System Models (ESMs) ~~, as~~ is used. It is therefore essential that ESMs are able to realistically simulate the SMB. This is specifically challenging, as ESMs exhibit biases and the horizontal resolution is often not sufficient to capture small scale climate features, e.g., sharp topographic gradients at the ice sheet margins as well as cloud, snow and firn processes (e.g., Lenaerts et al., 2017; van Kampenhout et al., 2017; Fyke et al., 2018).

In this study, SMBs are derived from transient simulations of the last deglaciation with the Max Planck Institute ESM (MPI-ESM) using an energy balance model (EBM). The EBM accounts for the energy balance at the surface, including snow processes, such as albedo evolution or refreezing and has been shown to result in a more realistic representation of ice volume changes than other methods (e.g., positive degree day models)(e.g., Tarasov and Richard Peltier, 2002; Abe-Ouchi et al., 2007; Bauer and C
. To thoroughly evaluate the SMBs derived with this setup, the EBM is also applied to MPI-ESM simulations of the recent historical period (1980–2010) and compared to Greenland SMBs from regional modeling. ~~Therefore, most of the analyses on changes and variability of the SMB have been based on observations, statistical regression and correction techniques as well as simulations with high-resolution regional climate models and covered the last century only (e.g., Fettweis et al., 2008; Ettema et al., 2009; I~~
~~.~~

This study extends the analysis of northern hemisphere SMB changes to the last deglaciation (~~21 thousand years (ka) before present (BP) to the~~ 21 ka to present). The last deglaciation was characterized by significant changes in insolation and associated changes in ~~ice sheets,~~ greenhouse gas concentrations, ice sheets, and other amplifying feedbacks (Clark et al., 2012). The large ice loss resulted in the disappearance of the North American and Eurasian ice sheets. In the Northern Hemisphere, only the Greenland ice sheet remains at present. The retreat of the ice sheets during the deglaciation resulted in about ~~1 m~~ 1 m sea-level rise per ~~100 years~~100 years, a rate, which on average is comparable to future projections of sea-level rise (e.g., Horton et al., 2014). The collapse of the ice sheets also resulted in significant changes in the atmospheric and oceanic circulation as well as associated climate features (e.g. Löfverström and Lora, 2017). Orographic changes, induced by the decrease of the Laurentide and Cordilleran ice sheets, led to changes in the Northern Hemispheric stationary wave patterns and thereby the North Atlantic jet stream, which significantly affected the northern hemispheric climate (e.g. precipitation and temperature patterns) (Andres and Tarasov, 2019; Löfverström, 2020; Kageyama et al., 2020). Superimposed on these ~~overall~~ long-term changes were periods of abrupt climate events. Some of the most prominent events are Heinrich event 1 (HE1; about ~~16.8 ka BP) (e.g., McManus et al., 2004; Stanford et al., 2011)~~ 16.8 ka) (e.g., Heinrich, 1988; McManus et al., 2004; Stanford et al., 2011) and the Younger Dryas (about ~~13-11.5 ka BP~~13 ka–11.5 ka)(Carlson et al., 2007), both associated with a major Northern Hemispheric cooling and a significant decrease of the Atlantic ~~Overturning Circulation.~~

~~To explore the SMB under such climate conditions, transient simulations of the last deglaciation with a comprehensive ESM are used in combination with an energy balance model (EBM) to calculate the SMB. An EBM approach is computationally more expensive as compared to other models (e.g., positive degree day models)(e.g., Tarasov and Richard Peltier, 2002; Abe-Ouchi et al., 2~~ ~~, as EBMs account for the energy balance at the surface, including snow processes, such as albedo evolution or refreezing. Hence, they mainly have been mainly for shorter-term simulations such as future predictions (Fettweis, 2007; Fettweis et al., 2013; Ettema e~~ ~~. However, using different approaches to calculate the SMB in simulations of the last glacial cycle with an intermediate complexity model, Bauer and Ganopolski (2017) have shown that only the EBM approach results in~~ Meridional Overturning Circulation (e.g. Keigwin and Lehman, 1994; Vidal et al., 1997). These climate changes and the variability associated with the changes in the northern hemispheric ice sheets during the deglaciation and the resemblance to the expected future climate change emphasize the need for a realistic representation of ~~ice volume changes~~the SMB for past and future stand-alone ice sheet and coupled climate-ice sheet model simulations (Fyke et al., 2018).

The main aim of this paper is to introduce the EBM and apply it to ~~long term~~ long-term climate simulations. First, we introduce the EBM and the underlying simulations with the ~~Max Planck Institute ESM (~~MPI-ESM~~)~~. Second, we provide a thorough evaluation of the model performance for present-day climate conditions over Greenland, by comparing the derived SMB data set to SMBs from regional climate modeling. We then present and investigate ~~SMB~~ changes and variability in the SMB and Equilibrium Line Altitude (ELA) throughout the last deglaciation and point out mechanisms behind the SMB ~~changes.~~ and ELA changes. Here, we aim at exploring SMB and ELA changes under a transient climate forcing in order to understand the mechanisms behind their variability on glacial time scales. A thorough evaluation of the long-term model simulations and their forcing data sets used here is subject to a future study. As the SMB is a key parameter in controlling changes in the geometry of the ice sheets, this data set will be made available to the ice-sheet modeling community along with other forcing fields required for ice-sheet model simulations.

2 Model Systems and Data

To obtain SMB fields from long-term climate simulations the coupled MPI-ESM is used in combination with ~~a~~ an EBM. Two ~~kind~~ kinds of simulations were performed: 1) A set of historical simulations (1980–2010) to evaluate the EBM derived SMBs. For this, we force the EBM with output from historical simulations with MPI-ESM as well as ERA-Interim reanalysis and compare the obtained SMBs to ~~SMBs derived with~~ output from the regional climate model MAR (Modèle Atmosphérique Régional) (Fettweis, 2007); 2) Simulations of the last deglaciation with prescribed ice sheet boundary conditions to investigate SMB changes under transient climate forcing. The simulations performed for this study are summarized in Table 2.

2.1 The Surface Energy and Mass Balance Model

We use the EBM to calculate and downscale the SMB from the coarse resolution atmospheric model grid onto high-resolution ice-sheet topographies. The main challenge in downscaling the SMB is to realistically capture the small scale features of both melt and accumulation. Melt and accumulation are highly dependent on the topographic height, e.g., at a given time, low elevations might experience melt while higher elevations remain frozen. Projecting melt and accumulation on a topography with better resolved vertical gradients has therefore a significant impact on the SMB. ~~Differences~~ Hence, differences between the original and downscaled SMBs are ~~therefore~~ mainly a result of differences in the elevation rather than the horizontal grid refinement. To account for this, we employ a 3-D EBM scheme that is forced with high-frequency atmospheric data. The EBM scheme is an enhanced version of the energy and mass balance code that has been used to couple the ice sheet model SICOPOLIS to a previous version of MPI-ESM (Mikolajewicz et al., 2007; Vizcaíno et al., 2008, 2010). The main improvements are 1) an advanced broadband albedo scheme considering aging, snow depth dependency, and the influence of the cloud coverage on the thermal radiation, 2) the consideration of ~~vertical movement of the~~ snow compaction and the vertical advection of snow/ice properties~~and compaction~~, 3) rain-induced change of the heat content of the snow layers, and 4) an enhanced refreezing scheme. We further adopted the scheme by introducing elevation classes~~. They were first introduced by Vizcaíno et al. (2013) within the CESM-Glimmer model setup and have~~ , following Lipscomb et al. (2013). Calculating the SMB on fixed elevation levels, has the advantage that the model becomes computationally cheaper, as the SMB is computed on the native and coarse resolution atmospheric grid instead of the high-resolution ice sheet topography. The obtained 3-D fields can be interpolated onto different ice sheet topographies (see Section 2.3). Note, that an elevation dependence of the SMB components is a simplified assumption and valid mainly for present-day Greenland. Atmospheric dynamics also significantly contribute to variations in the SMB components, specifically over present-day Antarctica. In the following, we present the basic structure of the EBM, including its improvements as compared to the scheme used in Vizcaíno et al. (2010).

Height correction

To compute the SMB, atmospheric fields are mapped onto 24 fixed elevation levels, ranging from sea level to ~~8000 m~~ $8000\,\mathrm{m}$ (we use irregular intervals that start with ~~100 m~~ $100\,\mathrm{m}$ distance at the surface and increase with height; see Table A1). To account for height differences between each of these elevation classes and the surface elevation of the atmospheric model, a height correction is applied to near-surface air temperature, humidity, dew point, precipitation, downward longwave radiation, and near-surface density fields. The downward shortwave radiation is kept constant, as it is largely affected by atmospheric properties independent of elevation differences (e.g., ozone concentration, aerosol thickness) (Yang et al., 2006).

The following height corrections are applied before the EBM calculations:

– ~~Precipitation rates~~ Total precipitation rates (liquid and solid) are corrected under consideration of the height-desertification effect. This halves the precipitation for an orography height difference of ~~1000 m~~ $1000\,\mathrm{m}$ above a threshold height of ~~2000 m~~ $2000\,\mathrm{m}$ for each grid point ~~(?).~~ (Budd and Smith, 1981). Note, that snowfall is determined from the total precipitation for height corrected near-surface air temperatures below $0\,^{\circ}\mathrm{C}$ within the EBM.

– Near-surface air temperature and dew point are corrected using a constant lapse-rate of ~~-4.6 K km^{-1}~~ $-4.6\,\mathrm{K\,km^{-1}}$, similar to the value proposed in Abe-Ouchi et al. (2007). The specific humidity, which can be used alternatively to the ~~dew point~~ height corrected dew-point temperature to calculate the latent heat flux (Bolton, 1980), is decreased with height, under the assumption that the relative humidity stays constant throughout the atmospheric column.

– The surface pressure is adjusted under the assumption of a typical atmospheric density/pressure profile $p = p_{\mathrm{atm0}} \exp\left(\frac{-z}{H_s}\right)$, where p_{atm0} is the pressure at the surface, z is the height and H_s the scale height with a typical value of ~~8.4 km~~ $8.4\,\mathrm{km}$.

– The downward longwave radiation is corrected by applying the observed constant radiation gradient of Marty et al. (2002) and is reduced by ~~29 W m^{-2} km^{-1}~~ $29\,\mathrm{W\,m^{-2}\,km^{-1}}$ (see also Wild et al., 1995).

Surface mass and energy balance calculation

Accumulation and melt determine the SMB. Precipitation is accumulated and falls as snow with a density of ~~300 kg m^{-3}~~ $300\,\mathrm{kg\,m^{-3}}$ when the height-corrected near-surface air temperature is lower than the freezing temperature of ~~273.15 K~~ $273.15\,\mathrm{K}$. Otherwise, precipitation falls as rain.

The computation of melt requires a snow/ice model, as the melt rate depends on the heat content of snow and the heat exchange between the surface snow layer and the atmosphere above as well as the snow/ice layers below. To account for this, the EBM consists of a 5-layer snow model, discretized into layers of increasing thickness. The model considers only vertical exchanges because the horizontal extent is several orders of magnitude larger than the vertical extent. The snow model starts initially with a reference density describing the typical exponentially increasing density with depth (Cuffey and Paterson, 2010). The top layer's exchange with the atmosphere is computed from short- and longwave radiation fluxes, latent and sensible heat fluxes, and the heat release due to the immediate refreezing of rain, if the surface layer has a temperature below the freezing temperature. Latent and sensible heat fluxes are parameterized and calculated from the height-corrected variables. The temperature of rain is assumed to be equal to the height-corrected near-surface air temperature. After updating the heat content of the surface layer, the temperature difference with the layer below determines the heat flux into the layer below by taking an ice/snow density-dependent heat conductivity into account (Fukusako, 1990). The heat conductivity is a function of density following Schwerdtfeger (1963), where the conductivity of ice is $K_{\mathrm{ice}} =$ ~~2.10 Wm^{-1} K^{-1}~~ $2.10\,\mathrm{Wm^{-1}\,K^{-1}}$, a common value within the reported range from ~~2.09 Wm^{-1} K^{-1} to 2.26 Wm^{-1} K^{-1}~~ $2.09\,\mathrm{Wm^{-1}\,K^{-1}}$ to $2.26\,\mathrm{Wm^{-1}\,K^{-1}}$ (Yen, 1981). We neglect any temperature dependence of the ice and snow conductivity (Fukusako, 1990). The scheme progresses downward until the lowest layer is updated. The heat flux beyond the lowest layer is assumed to be zero, in agreement with observations showing that the ice/snow layer temperature below 10 m follows the long-term trend and not the seasonal cycle. If the ice/snow layer's temperature exceeds the melting temperature, the temperature is set to the freezing point, and the related temperature excess converts the corresponding amount of ice/snow into liquid water. Liquid water penetrates into the layer below and refreezes in this layer as long as the layer is colder than the freezing temperature. Any remaining liquid water may penetrate further downward, where it potentially refreezes. Liquid water that leaves the lowest layer or flows into a layer with a density exceeding the pore close density of ~~830 kg m^{-3}~~ $830\,\mathrm{kg\,m^{-3}}$ (Pfeffer et al., 1991) is treated as run-off. Rain that precipitates on the surface refreezes in the surface layer by releasing latent heat. It increases the surface temperature until the surface reaches the melting point, which terminates refreezing. Henceforth, rain percolates into the layer below, where it is treated as meltwater.

Albedo

The amount of incoming radiation, which is available for heating the snow/ice layers and eventually melting, is controlled by the surface albedo α. The albedo parametrization used here differs from Vizcaíno et al. (2010). We have developed a frequency-independent broadband albedo that combines existing parameterizations, as described in this section. It represents processes neglected in conventional parameterizations and covers a broader range of albedos suggested by observational accounts. Note that all depths presented in the following are water equivalent (WE) depths (reference density of $1000\,\mathrm{kg\,m^{-3}}$).

Freshly fallen snow has (in our scheme) an albedo of 0.92 (α_{frsnow}, see Table 1). Snow metamorphosis processes that change the snow's characteristics through the growth of larger crystals at the expense of smaller ones, ultimately transform snow into firn (Cuffey and Paterson, 2010). As a result the snow albedo ($\alpha_{snow}(t)$) decreases and approaches the albedo of firn (α_{firn}), which is parameterized by a time-dependent exponential decay (Klok and Oerlemans, 2004; Oerlemans and Knap, 1998) as

$$\alpha_{snow}(t) = \alpha_{firn} + (\alpha_{frsnow} - \alpha_{firn})\exp(-t_{snow}\hat{\tau_a}), \tag{1}$$

where t_{snow} is the time since the last snowfall and $\hat{\tau_a}$ a time constant (see Table 1). This process is here referred to as "aging". Besides, the depth of the top snow layer ($d_{snow}(t)$) determines how much of a potentially darker background shines through and modulates the surface albedo (Klok and Oerlemans, 2004; Oerlemans and Knap, 1998). The equation

$$\alpha_{surface}(t, d_{snow}) = \alpha_{snow}(t) + (\alpha_{bg} - \alpha_{snow}(t))\exp(d_{snow}/\hat{d}), \tag{2}$$

renders this process, where α_{bg} is the background albedo, which is generally the albedo of ice, and $\hat{d}$ is ~~0.0024 m^{-1}~~ $0.0024\,\mathrm{m}^{-1}$. In the albedo parameterization melting reduces the snow thickness while snowfall increases the thickness when the precipitation rate exceeds ~~$7.23 \cdot 10^{-10}$ m(WE) s^{-1}~~ $7.23 \cdot 10^{-10}\,\mathrm{m(WE)\,s^{-1}} \approx$ ~~2.5 cm(WE) $year^{-1}$~~ $2.5\,\mathrm{cm(WE)\,year^{-1}}$; all depths presented here are water equivalent (WE) depths (reference density of ~~1000 kgm^{-3}~~ $1000\,\mathrm{kg\,m^{-3}}$). The maximum snow depth is set to ~~2 m WE~~ $2\,\mathrm{m(WE)}$, which corresponds to approximately ~~6 m~~ $6\,\mathrm{m}$ of snow. Any additional snow is still considered in the layer model to close the mass calculation but it does not impact the albedo (the snow depth is an internal diagnostic variable).

Depending on the snow depth, melting and refreezing have different albedo values. When the surface experiences melt, the albedo drops to the melt albedo of snow or ice, respectively. When the surface refreezes, the albedos ~~brighten~~increase, and the aging process starts. Compared to snow processes, the albedo differences for refrozen surfaces are smaller, and the process is slower ($\hat{\tau}_{ar}$ for refrozen snow and ice, Table~~1~~ 1???). Depending on the snow depth, their albedos start from the refrozen values of snow ($\alpha_{snow:refrz}$) or ice ($\alpha_{ice:refrz}$). Only melted surfaces and the background do not experience any aging.

Moreover, the background albedo shows a slight density dependence, which impacts regions of persistent high melting and lowers the surface albedo via the background albedo (Eq~~2~~ 1???). The background albedo is

$$\alpha_{bg} = \min(\alpha_{ice}, q_1\rho + q_2), \tag{3}$$

where q_1 = ~~$-4{\cdot}10^{-4}$ m^{3}kg^{-1}~~ $-4 \cdot 10^{-4}\,\mathrm{m}^3\,\mathrm{kg}^{-1}$ and q_2 = ~~0.95~~ 0.95, which is similar to values published by Liston et al. (1999); see also Suzuki et al. (2006) as another example for this kind of parameterization.

Furthermore, varying cloud cover affects the surface albedo (Greuell and Konzelmann, 1994a) because a higher cloud cover reflects more thermal radiation downward, which shifts the broadband albedo towards lower values (darker surface). We use the linear function of Greuell and Konzelmann (1994b) so that the maximum albedo change is 0.1 between a complete overcast sky and cloud-free conditions.

All albedo values used in this study (e.g., for refrozen snow/ice, fresh snow, ice, firn) are tuned for a realistic representation of the SMB for historical climate conditions (see Section 3) and are listed in Table 1. The same parameters were applied in an EBM simulation forced with output from a high resolution MPI-ESM simulation for historical climate conditions within the scope of a SMB model inter-comparison (SMBMIP Fettweis et al., 2020). The results showed that the derived SMBs were very similar to observations in terms of the SMB mean climate as well as the SMB trend (2003–2012).

Vertical advection and density evolution

Adding snowfall and releasing meltwater drives the movement of mass through the column, which, ultimately, drives the compaction of snow. In contrast to commonly used equations that diagnose snow compaction, we apply a simple parameterization. ~~By construction, it reproduces a defined density depth profile perfectly if snow is added to the snow column at the top while melting is absent. Our reference density profile increases exponentially with depth (Cuffey and Paterson, 2010). Parallel to the movement of mass, the corresponding temperature profile also shifts.~~

~~Our scheme handles two cases: 1) where surface melting subtracts mass from the top layer or 2) where~~ In the case of accumulation, snowfall adds mass ~~at the top. The~~ with a temperature of the height corrected near-surface air temperature to the top layer. For each layer, the inflow of snow and ice from above is added to ~~each~~ the layer by increasing the layer's density until it reaches the reference density of this layer. ~~Any additional inflow from above bypasses the layer and is redirected into the layer below. Once~~ This process repeats for each layer until mass flows out of the bottom layer ~~, it leaves the system.~~ and the mass is removed from the system. The parameterization uses a defined density depth profile, which increases exponentially with depth (Cuffey and Paterson, 2010). It reproduces this reference profile perfectly by construction if snow is added to the snow column at the top while melting is absent. The evolution of the temperature profile follows the movement of mass, applying a 1-d advection equation.

In the case of ~~surface melting, the entire density profile is lifted upward by the corresponding amount~~ablation, which is assumed to occur at the surface, the density and temperature profiles are shifted upwards by the thickness of the melted layer. An inflow of ~~mass~~ ice through the bottom layer closes the mass budget. The ~~inflow has a density of a virtual layer beneath the bottom box.~~

~~In each layer , the entry of freshwater~~ result is a density profile with a density in each layer between the reference density and the density of ice. The downward percolation of liquid melt or rain water into a layer can potentially increase the local density. The freshwater entered from above refreezes ~~if the layer 's~~ in each layer if its temperature is colder than the freezing point temperature~~, as described above~~. Water refreezes as ice with a density of ~~917 kg m^{-3}~~ $917\,\mathrm{kg\,m^{-3}}$. As a consequence, the layer's density grows ~~and eventually exceeds the layer's reference density ; here, it occurs without triggering any mass exchange beyond the~~ under consideration of mass conservation and eventually reaches the density of ice. Further, refreezing of melt or rain water heats the ice layer, bringing the layer~~. Although the mass entering the lowest layerfrom below is lower than the density of ice, in ablation areas, sustained refreezing increases gradually the density of layers by refrozen freshwater. Once the pore closure density is reached, it prevents further percolation into deeper layers~~'s temperature closer to the freezing point temperature. If the pore close off density of ice is reached (830 kg m^{-3}; Pfeffer) in one layer, further downward percolation stops, and the remaining melt water runs off and leaves the system.

2.2 The Max Planck Institute Earth System Model

The simulations in this study are performed with the Max Planck Institute for Meteorology Earth System Model (MPI-ESM, version 1.2; see Mikolajewicz et al., 2018; Mauritsen et al., 2019), consisting of the spectral atmosphere general circulation model ECHAM6.3 (Stevens et al., 2013), the land surface vegetation model JSBACH3.2 (Raddatz et al., 2007) and the primitive equation ocean model MPIOM1.6 (Marsland et al., 2003). Two different resolutions are used for the simulations. 1) For calculating the SMB over the last deglaciation, MPI-ESM is used in its coarse resolution (CR) setup, hereafter referred to as MPI-ESM-CR. In this setup ECHAM6.3 has a T31 ~~spectral~~ horizontal resolution (approx. ~~3.75°~~ 3.75°) with 31 vertical hybrid σ-levels, which resolve the atmosphere up to ~~0.01 hPa~~ 0.01 hPa (Stevens et al., 2013), and MPIOM1.6 has a nominal resolution of ~~3°~~ 3°, with two poles located over Greenland and Antarctica (Mikolajewicz et al., 2007). The selected setup is a compromise between computational feasibility and model resolution. 2) We additionally use simulation with the low resolution version of MPI-ESM1.2, hereafter referred to as MPI-ESM-LR, where ECHAM6.3 has a T63 spectral (approx. ~~1.88°~~ 1.88°) grid with 47 vertical levels and MPIOM features a ~~1.5°~~ 1.5° nominal resolution. For model details see Mauritsen et al. (2019).

2.3 Transient Climate Simulations

MPI-ESM Experimental Designs

We performed different simulations with the MPI-ESM-CR setup: 1) simulations to investigate the SMB throughout the last deglaciation, starting ~~26 ka BP until present ,~~ 26 ka before present until present (here, defined as 1950), and 2) simulations to evaluate the SMB for historical climate conditions (see Table 2). For the deglaciation experiment, the model was started from a spun-up glacial steady state and integrated from ~~26 ka BP~~ 26 ka until the year 1950, with prescribed atmospheric greenhouse gases (Köhler et al., 2017) and insolation (Berger and Loutre, 1991). The ice sheets and surface topographies were prescribed from the GLAC-1D (Tarasov et al., 2012; Briggs et al., 2014) reconstructions (Kageyama et al., 2017, see standardized PMIP4 experiments). ~~The first 5 ka of this simulation are considered as spin-up, and we~~ We focus our analysis on the last ~~21 ka~~ 21 ka of the simulation. Hereafter, this simulation is referred to as MPI-ESM-CR deglaciation experiment. All forcing fields are ~~updated every 10 years~~ prescribed every 10 years and initiate changes of the topography and glacier mask, as well as modifications of river pathways, the ocean bathymetry and the land-sea mask (Riddick et al., 2018; Meccia and Mikolajewicz, 2018). Freshwater from changing ice sheets is calculated from the thickness changes in the ice-sheet reconstructions for each grid point. For grid cells over land melt water is distributed through the hydrological discharge model, over ocean it is discharged into the adjacent ocean grid cells. Land cells that are deglaciated are covered with the same vegetation form as the adjacent grid cells. Anthropogenic forcing, such as land use, is turned off in this simulation. For calculating the SMB, relevant variables of the atmospheric component of MPI-ESM1.2 are written out hourly throughout the simulation. Using the obtained atmospheric fields within the EBM (see Section 2.1) results in 3-D SMB fields, which are then interpolated onto the GLAC-1D topography and ice mask (Tarasov et al., 2012). Computing a 3-D SMB also allows us to calculate the equilibrium line altitude (ELA), the elevation at which the SMB equals zero. ~~Above this altitude~~ At heights above the ELA it is thermodynamically possible to accumulate snow throughout the year and form an ice sheet or glacier. ~~The ELA is less sensitive to changes in the ice sheet mask and less dependent on the surface topography than the SMB; hence, it is a good~~ At elevations below the ELA melt dominates accumulation and no ice sheet can form. Here, the ELA is calculated in each grid point, hence, resembles a potential ELA. It is a proxy for climate changes affecting the ice sheets. As the ELA estimate is calculated on the native model grid it is more consistent with the model physics and boundary conditions used in the simulations than the downscaled SMB. Hence, integrated values of the ELA are less sensitive to changes in the ice-sheet mask than those of the SMB.

For the evaluation of the derived SMBs under historical climate conditions, we branched off ~~the~~ a last millennium simulation at ~~950 a BP~~ 950 a BP (years before present) from the deglaciation experiment. Topography, land-sea and glacier masks, river pathways, and the ocean bathymetry are taken from the deglaciation experiment and kept constant at ~~950 a BP~~950 a BP. Other forcing fields are adopted according to the PMIP3 standard protocol for the Last Millennium simulations (Schmidt et al., 2012) and updated every year. The forcing fields for the years 1850 to 2010 are taken from the CMIP6 simulations (see Mauritsen et al., 2019). For the years beyond 2010, the forcing fields in the desired resolution were not available at the time of the analysis. Overall, the applied forcing allows for a more realistic treatment of atmospheric processes associated with changes in e.g., ozone, aerosols, CO_2 concentrations, and land use, and it accounts for their climatic impacts for present day climate conditions. Specifically, we apply time-varying greenhouse gases (CO_2, N_2O, CH_4), volcanic forcing, ozone, tropospheric aerosols and land-cover changes (see Jungclaus et al., 2010; Mauritsen et al., 2019). For the evaluation only the years 1980–2010 are used, which allows for a ~~long enough~~ sufficient adjustment of the model to changes in the forcing. We hereafter refer to this simulation as the MPI-ESM-CR historical experiment. Note, that changes in the topography due to ice sheets are small between 950 a BP and 2010. Hence, we expect only a minor impact on the obtained SMBs.

Additionally, we performed a deglacial, last millennium, and historical simulation where ice sheets and topographies are prescribed from ICE-6G ~~(Peltier et al., 2015; ?) reconstructions~~ reconstructions (Peltier et al., 2015), an alternative reconstruction often used as boundary forcing in deglacial simulations (Kageyama et al., 2017). Results from these simulations, hereafter referred to as MPI-ESM-CR$_{\mathrm{Ice6G}}$ experiments, are shown in Appendix A1 and emphasize differences in the SMB and relevant fields due to different ice-sheet boundary conditions. While the SMB response to the climate forcing in these simulations is qualitatively similar to the MPI-ESM-CR simulations forced with GLAC-1D reconstructions, differences in the freshwater runoff between the reconstructions lead to a different climate response in the model simulations.

For a thorough evaluation of the EBM and in order to investigate the effect of model resolution on the historical SMB, we additionally calculate the 3-D SMB fields from a CMIP6 (Wieners et al., 2019) historical simulation with the MPI-ESM-LR setup (see Section 2.2) (Mauritsen et al., 2019; Wieners et al., 2019). The simulation allows to further evaluate the EBM and to investigate differences in SMBs in regards to the spatial model resolution as well as differences due to the underlying topographies. This simulation is hereafter referred to as MPI-ESM-LR historical experiment.

The 3-D fields derived for all historical control simulations are 3-dimensionally interpolated onto the ISMIP6 topography and masked with the ISMIP6 ice mask ~~(see Section ?? Nowicki et al., 2016; Fettweis et al., 2020)~~(see Section 2.3 Nowicki et al., 2016; Fettwe
.

~~ERA-Interim Reanalysis~~Evaluation Data

To evaluate the EBM with respect to the atmospheric forcing data and its resolution, we additionally force the EBM with ERA-Interim reanalysis data from the European Center for Medium-Range Weather Forecasts (ECMWF, Dee et al., 2011). For comparison, we also interpolate the ERA-Interim derived 3-D SMB fields onto the ISMIP6 topography and masked with the ISMIP6 ice mask (see Section 2.3). ERA-Interim is available as 6-hourly data on a ~~0.75°x0.75°~~ $0.75° \times 0.75°$ horizontal resolution. ERA-Interim assimilates a great fraction of in-situ and remote sensing observations, making it one of the best reanalysis products available (Cox et al., 2012; Zygmuntowska et al., 2012). However, as reanalysis data sets are model products, they exhibit biases specifically for variables associated with small-scale processes ~~, e.g., clouds,~~ and areas where in-situ observations are sparse (Stengel et al., 2018) ~~.~~ (e.g. precipitation, clouds). These biases are not unique to the ERA-Interim but can be found in other reanalyses (Miller et al., 2018). Relevant biases for this study are discussed in Section 3.

~~The Regional Model MAR~~

~~For evaluation~~Additionally, we compare the obtained SMB data sets from the MPI-ESM historical experiments to SMBs derived with the regional climate model MAR (Modèle Atmosphérique Régional, version 3.9.6). For a detailed description of MAR and its setup, see Fettweis et al. (2017, 2020). The MAR simulation used in this study was run on a ~~15 km~~ 15 km horizontal resolution with ERA-Interim boundary forcing (Dee et al., 2011) and interpolated onto the ~~ISMIP~~ ISMIP6 topography (Nowicki et al., 2016), as described in Fettweis et al. (2020).

3 The Greenland Surface Mass Balance Under Historical Climate Conditions

For the Greenland ice sheet, a thorough evaluation of the accumulation and surface energy budget that determines surface melt is conducted under historical climate conditions (1980–2010). Variables derived from the EBM simulations forced with output from ERA-Interim and the historical MPI-ESM1.2 simulations are compared to SMBs from MAR. SMB, accumulation and melt data sets are presented on the same ~~ISMIP~~ ISMIP6 topography (see Section ~~??).~~ 2.3). In the following, accumulation is defined as mass gain due to snow deposition and melt as mass loss due to ablation (often referred to as runoff). Refreezing processes are considered in the melt estimate (see Section 2.1). All variables obtained using the EBM are hereafter referred to as $\mathrm{EBM_{MPI-ESM-CR}}$, $\mathrm{EBM_{MPI-ESM-LR}}$, and $\mathrm{EBM_{ERAI}}$ for the EBM simulations forced with the historical simulations of both ~~MPI-ESM-CR and MPI-ESM-LR~~MPI-ESM in coarse (CR) and low (LR) resolution, and ERA-Interim reanalysis. The annual mean SMB averaged over 1980–2010 and the Greenland integrated value are shown in Figure 1 and Table 3 for each of the simulations. The corresponding plots for the MPI-ESM-CR$_{\mathrm{Ice6G}}$ simulation are shown in Fig. A1.

The SMBs from EBM$_{\mathrm{ERAI}}$, EBM$_{\mathrm{MPI-ESM-LR}}$, and EBM$_{\mathrm{MPI-ESM-CR}}$ show good agreement with SMBs from MAR for the historical period. The largest mass loss occurs along the low elevation areas close to the coasts, with maxima in the west and southwest of Greenland. The largest mass gain is evident in the higher elevation areas in the west and southeast of Greenland. For all simulations, the mass changes over northern central Greenland are small, due to low precipitation at high elevations (see Fig. 2). Also, the gradients between areas of most pronounced mass loss and gain are qualitatively similar in all simulations. Differences in the SMB fields are largest along the coasts in the southeast and west of the Greenland ice sheet. These differences are likely a result of the forcing data, model resolution (about ~~3.75°~~ 3.75° – approx. ~~400 km at the Equator –~~ 250 km over Greenland for MPI-ESM-CR, ~~1.88°~~ 1.88° – approx. ~~210 km –~~ 120 km for MPI-ESM-LR, ~~0.75°~~ 0.75° – approx. ~~80 km –~~ 50 km for ERA-Interim, and ~~15 km~~ 15 km for MAR) and underlying topographies (Fig. 2). Differences between MAR and EBM$_{\mathrm{ERAI}}$ are generally smaller than differences between MAR and EBM$_{\mathrm{MPI-ESM-CR}}$ or EBM$_{\mathrm{MPI-ESM-LR}}$ because ERA-Interim data were used as boundary forcing for the MAR simulation. Comparing SMBs derived from EBM$_{\mathrm{MPI-ESM-CR}}$ and EBM$_{\mathrm{MPI-ESM-LR}}$ shows that specifically the SMB differences in the North of the Greenland ice sheet, associated with more melt in EBM$_{\mathrm{MPI-ESM-CR}}$ along the coasts and enhanced accumulation in the center of the ice sheet as compared to EBM$_{\mathrm{MPI-ESM-LR}}$, are ~~likely~~ partly a consequence of the model resolution. In the following we investigate the components that determine the SMB individually to understand the mentioned differences between the simulations better.

Accumulation

Accumulation patterns in MAR and the three EBM simulations are similar. However, they show some differences in the low elevation areas in the southeast of the ice sheet and the northern plateau (Fig. 1). Integrated over the ice sheet, EBM$_{\mathrm{ERAI}}$, EBM$_{\mathrm{MPI-ESM-CR}}$, and EBM$_{\mathrm{MPI-ESM-LR}}$ simulate lower accumulation than MAR as well as ~~RACMO (~~the Regional Atmospheric Climate Model (RACMO, Table 3). This difference is associated with less snowfall and more rainfall in ERA-Interim and the two MPI-ESM simulations than in the regional models, specifically in the low elevation areas along the coastal areas of Greenland (Fig. 2). The underestimation of ERA-Interim's snowfall that extends into the high elevation areas of the ice sheet is likely associated with an unrealistic representation of clouds and a low cloud bias as well as shortcomings in modeling seasonal changes in surface temperatures (see Section Melt; Miller et al., 2018). In the higher elevation areas of most of the central parts of Greenland MPI-ESM-CR and MPI-ESM-LR overestimate snowfall, which is tightly linked to topographic differences underlying the models as well as model biases in the atmospheric circulation patterns affecting precipitation (Fig. 2) (Mauritsen et al., 2019). Areas that are lower in MPI-ESM-CR and MPI-ESM-LR than MAR, mainly due to the spectral smoothing in MPI-ESM, generally show more snowfall in the MPI-ESM simulations (Fig. 2). Comparing the accumulation derived from EBM$_{\mathrm{MPI-ESM-CR}}$ with EBM$_{\mathrm{MPI-ESM-LR}}$ shows that accumulation patterns in the southeast of the ice sheet are more confined towards the east coast but EBM$_{\mathrm{MPI-ESM-LR}}$ still features a significant underestimation of accumulation in the low elevation areas. Hence, the even higher resolution of MPI-ESM-LR is not sufficient to represent the regionally confined processes that determine the accumulation in these regions. The overestimation of accumulation in the North of the ice sheet is reduced in $\mathrm{EBM_{MPI-ESM-LR}}$ as compared to $\mathrm{EBM_{MPI-ESM-CR}}$~~, which~~. The reduction is likely associated with a better representation of the topographic gradients in the MPI-ESM-LR version of the model and an associated shift in precipitation patterns reducing precipitation at higher elevation. The comparison between $\mathrm{EBM_{MPI-ESM-LR}}$ and $\mathrm{EBM_{MPI-ESM-CR}}$ indicates that an increase in resolution cannot resolve all biases. This is in line with findings by van Kampenhout et al. (2019), showing that a regional grid refinement in simulations with the Community Earth System Model (CESM) did not improve all SMB components. Model biases, e.g. in the large-scale circulation, clouds and precipitation patterns (Mauritsen et al., 2019), as well as uncertainties due to internal variability are exhibited in all ESMs and explain part of the differences seen in the presented comparison.

Note, that the EBM calculates snowfall as precipitation at temperatures below ~~0°C~~ $0^\circ\mathrm{C}$ and partly compensates for these differences in snowfall and rainfall, specifically along the coastal areas in the west and southeast of the ice sheet (not shown). The seasonal differences are larger. In summer, ERA-Interim simulates less snowfall and more rainfall but shows slightly less total precipitation than MAR, which impacts the melt patterns (not shown).

Melt

$\mathrm{EBM_{MPI-ESM-CR}}$ shows significantly more surface melt along the western margins of the ice sheet than MAR (Fig. 1). These areas are topographically higher in MPI-ESM-CR than ~~in MAR~~ the ISMIP6 topography (Fig. 2). One problem of downscaling melt in these regions is that temperatures are always at the ~~melting~~ freezing point during melting. By projecting the temperatures onto lower elevations, the height corrected temperatures depart significantly from the ~~melting~~ freezing point towards higher temperatures. Hence, the vertical downscaling from higher elevations to low elevations overestimates melting. In contrast, the area in the south that is significantly higher than the ~~ISMIP~~ ISMIP6 topography shows less melt. It indicates that most of the differences are closely related to differences in the topography. Comparisons with $\mathrm{EBM_{MPI-ESM-LR}}$, which shows less melt in the north and west of the ice sheet as compared to $\mathrm{EBM_{MPI-ESM-CR}}$ (Fig. 1 and 2), confirm that differences in the melt patterns are linked to the underlying topographies of the model versions. MPI-ESM-LR is slightly higher than MPI-ESM-CR and thereby closer to MAR on the northern and western flanks of the ice sheet, hence $\mathrm{EBM_{MPI-ESM-LR}}$ shows less melt than $\mathrm{EBM_{MPI-ESM-CR}}$ in these areas. $\mathrm{EBM_{ERAI}}$ shows less melt in the southern and western parts of the ice sheets than MAR. These low melt rates are partly a result of the model tuning towards a similar integrated Greenland SMB value (see Table 3).

Heat fluxes towards the surface control predominately surface temperatures and melting. Miller et al. (2018), who compared surface energy fluxes over Greenland from different reanalyses with surface observations, found that Era-Interim largely underestimates downward longwave and shortwave radiation, likely associated with an unrealistic representation of cloud optical properties. Low surface albedos in ERA-Interim and an associated underestimation of outgoing shortwave radiation partially compensate for the downward longwave radiation deficit. Further, seasonal biases in the latent heat fluxes dampen the seasonal changes in surface temperatures. Such biases are not unique to the ERA-Interim but can also be found for other reanalyses (see Miller et al., 2018, for details) and models, such as MAR (Fettweis et al., 2017). We find similar biases in the $\mathrm{EBM_{MPI-ESM-LR}}$ simulation, which are likely associated with the simulated cloud cover.

4 SMB and ELA Changes Throughout the Last Deglaciation

The evaluation shows that ~~most of the discrepancies between the SMBs of~~ major differences between MAR and $\mathrm{EBM_{MPI-ESM-CR}}$ are the ~~result of differences in the model resolution and the underlying topography. Major differences are the~~ increased melt on the western flank of Greenland and along the coastal areas as well as the overestimation in accumulation in the southern part of Greenland, which ~~are largely a result of~~ can partly be reduced by increasing the model resolution, as shown by comparisons with $\mathrm{EBM_{MPI-ESM-LR}}$. Given these model limitations, the SMB is modeled well in comparison to MAR (or other regional models)(see also Fettweis et al., 2020) with the advantage of reduced computational costs that allow for a thorough investigation of the SMB for long-term climate simulations.

In the following we present the climate of the deglaciation experiment with MPI-ESM-CR based on Glac1D boundary conditions. ~~The scope of this paper is not to evaluate the model simulation nor the forcing data sets used here, e.g., the ice volume changes as prescribed by the Glac1D or Ice6G reconstructions. Rather, we aim at exploring SMB and ELA changes under a transient climate forcing in order to understand the mechanisms behind their variability on glacial time scales.~~ We limit the analysis to the Northern Hemispheric ice sheets only, with a specific focus on Greenland.

4.1 Greenland

As the SMB is highly dependent on the prescribed ice sheet geometry, it is challenging to interpret SMB changes for ice sheets that undergo substantial geometry changes throughout the deglaciation. As all northern hemispheric ice sheets except Greenland collapse entirely, we investigate the SMB evolution mainly for Greenland, where changes in the geometry were relatively small (Fig. 3, gray line in the top panel). Values for the SMB, ELA, accumulation, and melt integrated over Greenland are shown in Fig. 3. The SMB and ELA for six time slices of the deglaciation are shown in Fig ~~4~~. 4 in order to indicate the most drastic changes in the northern hemispheric ice sheet configuration.

Cold Northern Hemispheric temperatures during the LGM (approx. ~~21 to 19 ka BP~~ $21\,\mathrm{ka}$ to $19\,\mathrm{ka}$) are associated with a positive Greenland-wide integrated SMB of about ~~380 GT a^{-1}~~ $380\,\mathrm{GT\,a^{-1}}$. This SMB is dominated by accumulation while melt is close to zero (Fig. 3 and 4). This result is consistent with the Greenland ice sheet being close to its maximum extent during this period (Clark et al., 2009). Due to the increase in temperatures, following an increase in Northern Hemispheric summer insolation by approximately ~~7%~~ $7\,\%$ of the LGM value, and a simultaneous increase in the global CO_2 concentrations from ~~187 ppmv at 19 ka to 228 ppmv at 15 ka BP~~ $187\,\mathrm{ppmv}$ at $19\,\mathrm{ka}$ to $228\,\mathrm{ppmv}$ at $15\,\mathrm{ka}$, both accumulation and melt increase. The total accumulation over Greenland increases from about ~~420 Gt a^{-1}, at 19 ka BP~~ $420\,\mathrm{Gt\,a^{-1}}$, at $19\,\mathrm{ka}$, to about ~~670 GT a^{-1}, at 15 ka BP~~ $670\,\mathrm{GT\,a^{-1}}$, at $15\,\mathrm{ka}$ (more than ~~35%~~ $35\,\%$). The largest accumulation increase is evident over the south-western part of the ice sheets, which is associated with more precipitation (Fig. 5). Intriguingly, the increase in precipitation is not a uniform signal for the entire Northern Hemisphere but shows regional patterns, such as a decrease over parts of the North Atlantic and south of the Laurentide ice sheet edge. These patterns indicate that precipitation changes are not entirely thermodynamically driven (the atmosphere being able to hold more water with increasing temperatures) but points towards changes in the atmospheric dynamics. Melt increases from about ~~0 to 25 Gt a^{-1}~~ $0\,\mathrm{Gt\,a^{-1}}$ to $25\,\mathrm{Gt\,a^{-1}}$ between the

LGM and ~~15 ka BP~~15 ka. The growing melt is small and limited to the low elevation areas along the coast of Greenland. This growth is a consequence of increasing summer temperatures that exceed the freezing point in these areas and lead to enhanced melt during summer. In the other areas over Greenland, temperatures are, despite warmer summers, still too cold to trigger melt. As the increase in accumulation dominates enhanced melting, the SMB time series increases until about ~~15 ka BP~~ 15 ka (Fig. 3 and 4). Interestingly the ELA increases despite an SMB increase. Per definition, the ELA depends directly on shifts in areas of net melt and accumulation. Hence, it closely follows the increase in the ablation area. From the LGM to ~~15 ka BP~~ 15 ka the area of net ablation increases from ~~0 to about 58,400 km^2~~0 km^2 to about 58,400 km^2.

A simultaneous increase in SMB and ELA seems to be counter-intuitive at first, given that in a present-day climate, a decrease in SMB over Greenland is associated with an increase in the ELA and vice versa (e.g., Le clec'h et al., 2019). As the climate warms, the area of net ablation expands while the area of net accumulation ~~shrinks~~recedes, which moves the ELA upward. As melt is close to zero in the glacial climate, the SMB is dominated by the significant growth of accumulation due to warmer atmospheric temperatures and the associated increase in precipitation. The dominance of the accumulation in controlling the SMB explains the counter-intuitive behavior of the SMB and ELA in the glacial climate. Further, it ~~points towards the fact~~ suggests that changes in the ELA cannot be taken as a proxy for changes in the SMB.

At around ~~14.6 ka BP~~ 14.6 ka the SMB and ELA over Greenland decrease significantly for about ~~500 a~~500 a, the SMB drops from about ~~630 to 380 Gt a^{-1}~~ 630 Gt a^{-1} to 380 Gt a^{-1} and the ELA decreases from more than than ~~460 m to 120 m~~ 460 m to 120 m (Fig. 3). Regionally differences are even larger (Fig. 6). These drastic changes are associated with a significant reduction in the AMOC, as a response to increased inflow of freshwater from melting ice sheets into the global ocean as prescribed from the Glac1D ~~ice sheet~~ ice-sheet reconstructions. The strong melt-water pulse leads to a near-shutdown of the thermohaline circulation and a significant cooling of the North Atlantic and adjacent regions (Fig. 6). Although the largest cooling is occurring over the North Atlantic, the annual cooling signal extents over large regions of the Northern Hemisphere, including the Arctic Ocean, the North Pacific and large parts of Eurasia and North America (Fig. 6). Over Greenland, this cooling diminishes surface melt during summer, which is similar to LGM conditions. Again, the largest response is evident over the low elevation areas along the southern coasts of Greenland (see also Fig. 5 for similarities). Associated with the overall cooling is a decline in precipitation, which reduces accumulation by more than 40% over the ice sheet. Although melt and accumulation again partly compensate, accumulation changes occur over a much larger area and dominate changes in melt, so that the integrated SMB decreases for Greenland (Fig. 3).

After the recovery of the AMOC, at around ~~14 ka BP~~14 ka, the SMB declines and the ELA continues to move upward. Thereby it follows the overall warming signal as a response to increasing insolation and atmospheric greenhouse gases (Fig. 3 and 4). The decline in the SMB is associated with an overcompensation of the accumulation by a significant increase in melting. Thus, ELA and SMB are anti-correlated from about ~~14 ka BP~~ 14 ka onward and continue to increase and decrease, respectively. Only at around ~~13.6 ka and 11.6 ka BP~~13.6 ka and 11.6 ka, the ELA and SMB decrease significantly again, due to a second and third weakening of the AMOC. Similar to the first AMOC decline, the associated cooling of the North Atlantic and parts of Greenland leads to a decrease in accumulation, melt, and the ELA (Fig. 7). The changes are regionally very similar to the first event (Fig. 6). However, the Greenland integrated SMB shows a weaker signal in both cases than during the first freshwater event, as the changes in accumulation and melt partly compensate if integrated over the ice sheet (Fig. 3).

After the two AMOC events, the retreat of the Greenland ice sheet towards ~~his~~ its present-day state continues, associated with a decrease in SMB and an increase in ELA. The minimum SMB (~~216 Gt a^{-1}~~ 216 Gt a^{-1}) is reached at ~~8.7 ka BP~~ 8.7 ka, and the maximum ELA (1556 m) occurs at ~~9.3 ka BP~~ 9.3 ka (Fig. 3 and 4). Due to the continuing deglaciation, Greenland experiences its largest ice volume and extent changes between ~~10.8 ka and 9.1 ka BP~~ 10.8 ka and 9.1 ka (the ice sheet geometry influences SMB values during this period). At around ~~11.1 ka BP~~ 11.1 ka, the Northern Hemispheric summer insolation reaches its maximum and decreases continuously thereafter until the present, while the CO_2 concentration remains rather constant between ~~11.1 ka and 6 ka BP~~ 11.1 ka and 6 ka and slightly increases thereafter. Consequently, the ELA decreases, and the SMB begins to recover continuously after about ~~8.7 ka BP~~ 8.7 ka. Note, that a series of smaller AMOC weakening events is evident at around ~~10.1 ka, 8.4 ka, and 7.1 ka BP~~ 10.1 ka, 8.4 ka, and 7.1 ka, but their climate impact on the ELA and SMB does not manifest significantly in the time series for Greenland (Fig. 3). The ELA decrease and SMB increase continue until ~~200 a BP~~ 200 a BP despite a slight increase in the CO_2 concentration. These continuing changes suggest that the decreasing summer insolation drives SMB and ELA changes between ~~9 ka~~ 9 ka and 200 a BP. It is not before ~~100 a~~ 100 a BP that the ELA and SMB closely follow the CO_2 signal again. The sharp drop in the SMB and the uplift of the ELA for the last ~~100 years~~ 100 years of the simulation is similar to the warm period observed in the coastal temperatures of Greenland in the 1930s (Chylek et al., 2006). At the end of the simulation the ELA lies at about ~~1150 m~~ 1150 m and the SMB reaches values of ~~550 Gt a^{-1}~~ 550 Gt a^{-1}. These values are similar to values observed during the 21st-century, although slightly higher as no anthropogenic forcings are considered in the deglaciation simulation (see Fig. 4, Section 3 and Table 3; Box, 2013).

The SMB and ELA derived from the MPI-ESM-CR simulation with the prescribed Ice6G ice sheets are qualitatively similar to the presented results based on the Glac1D ~~ice sheet~~ ice-sheet reconstructions (see Fig. A2 to A6). The overall trends of both variables as well as the relationships between accumulation and melt (e.g. accumulation dominating melting until about 15 ka) are similar, but the timing of the weakening of the AMOC as well as the magnitude differ. These deviations are due to a different timing, magnitude and location of melt water release between the Glac1D and Ice6G reconstructions, which are currently investigated in a separate study.

4.2 Impact on the Eurasian and North American ELA

As discussed earlier, the North American (Laurentide and Cordilleran) and Eurasian (Fennoscandian, British Isles, and Barents-Kara Sea) ice sheets experience substantial changes in their glacial extent throughout the last deglaciation (Fig. 4). Reconstructions suggest a steady retreat of the Eurasian ice sheets starting from the LGM until about ~~9.7 ka BP~~ 8.7 ka, when the ~~last ice vanished from the continent~~ ice-sheets converged to present-day conditions over the continent (e.g. Patton et al., 2017). The decline is highly discontinuous and shows an acceleration at around ~~18.5 ka BP~~ 17.8 ka. Similarly, the extent of the North American ice sheet started to decrease shortly after the LGM and continued until about ~~6 ka BP~~ 6.8 ka, with only little ice left to the present day (e.g. Carlson et al., 2007). As the SMB is highly dependent on the ice sheet geometry, it is difficult to fully interpret SMB changes for the North American and Eurasian ice sheets. Hence, we only briefly point out the similarities between the climate responses of the ELAs over the North American, Eurasian, and Greenland ice sheets (see Fig. 5, 6 and 7) while keeping in mind that the interpretation is limited due to the extensive changes in the ice sheet geometries throughout the deglaciation. To account for the massive ice sheet changes in the time series, we split the ice sheets into different sub-regions and investigate their dependence on the ice sheet geometry. Fig. 8 shows the ELA time series for Eurasia, subdivided into a southern (~~<60°N~~< 60°N), central (~~60°–70°N~~60°N–70°N) and northern (~~>70°N~~> 70°N) ice sheet, and North America, split into a northern and southern Laurentide ice sheet (east of ~~120°W~~ 120°W and north of ~~60°N~~ 60°N and south of ~~60°N~~60°N, respectively) and a Cordilleran ice sheet (west of 120°W).

At the LGM, the average ELAs over Eurasia and North America are significantly higher than the ELA over Greenland for the same period, except for the North Eastern Laurentide and Northern Eurasian ice sheets (see Fig. 4 and 8). Similar to the Greenland ice sheet, the ELA increases continuously until about ~~15 ka BP~~ 15 ka for the Eurasian and North American ice sheets. At around ~~14.5 ka BP~~ 14.5 ka the southern and central Eurasian ice sheets both show a slight decrease in the ELA~~due to~~. This is likely associated with the AMOC slowdown (see Section 4.1); other AMOC events at around ~~19.6 ka, 18.2 ka, and 15.2 ka BP~~ 19.6 ka, 18.2 ka, and 15.2 ka also result in a decrease in ELA for the southern and central Eurasian ice sheet. However, the signal in the ELA is relatively weak and regionally confined compared to the response over Greenland. Around ~~14.5 ka~~ 14.5 ka the Eurasian ice sheet exhibits decreased ELAs on its western boundaries and the Laurentide ice sheet on its eastern boundaries since both melt and accumulation decrease in response to reduced North Atlantic temperatures (Fig. 6). This result suggests that the AMOC slowdown at ~~14.5 ka~~ 14.5 ka affected all ice sheets, at least regionally. ~~After this event, the~~ Another possible contributing factor to the pronounced SMB and ELA variability over the northern hemispheric ice sheets during this time period are changes in the atmospheric circulation. Löfverström and Lora (2017) found that elevation changes of the North American ice sheets around the saddle collapse, defined by the separation of the Laurentide and Cordilleran ice sheets, caused significant changes in the stationary wave patterns. An amplifying factor for atmospheric circulation changes is the southward extended sea-ice cover due to the AMOC slowdown and reduced North Atlantic sea-surface temperatures. Such changes have a significant influence on downstream precipitation and temperature patterns over the North Atlantic and adjacent areas.

After about 14 ka, the ELA continues to increase for nearly all ice sheets, following the overall warming signal. However, specifically for the southern ice sheets over Eurasia and North America the changes in the ice sheet extent have a large effect on the ELA. The signal in the ELA due to the changes in the ~~ice sheet~~ ice-sheet mask exceeds the signal due to the natural climate variability of the ELA at around ~~20.6 ka BP~~ 20.6 ka for the southern Eurasian ice sheet, about ~~18.9 ka BP~~ 18.9 ka for the northern Eurasian and southeast Laurentide, about ~~15.3 ka~~ 15.3 ka for the northern and central Eurasian and ~~13.3 ka~~ 13.3 ka for the Cordilleran ice sheet (Fig. 8). Hence, the second and third AMOC slowdowns are only poorly reflected in the ELA time series, although similar regional responses are evident in Fig. 7. By ~~9.7 ka BP~~ 9.7 ka Eurasia is completely ice free, while North America has only small ice sheets left (see Fig. 4).

5 Conclusions

In previous studies, changes and variability in SMB have been analyzed mainly for the last century, due to the availability of observations and the computational limitations of regional climate modeling. Here, we present the first analysis of SMB changes throughout the last deglaciation from a simulation with a comprehensive ESM. Despite the relatively low resolution of the MPI-ESM-CR simulation, used as forcing for the EBM, the obtained SMBs for historical climate conditions show good agreement with SMBs derived from regional climate modeling (see Table 3). A comparison with SMBs derived from a simulation with the MPI-ESM-LR setup and ERA-Interim reanalysis reveal that discrepancies between the SMBs derived from MPI-ESM-CR and MAR are a result of the coarse resolution of the model (e.g., the extensive melt in the North of the Greenland ice sheet) and due to the quality of the forcing itself (e.g., precipitation patterns). In contrast to ERA-Interim, MPI-ESM evolves freely and does not assimilate any surface observations; hence, differences are to be expected. Further differences are related to underlying topographies of the native models as well as the fact that most fluxes within the EBM are parameterized, as they are not directly available from the model simulations in the required temporal resolution. For example, several studies have pointed towards the specific importance of the albedo parameterization for a realistic simulation of the surface mass balance (e.g., van Angelen et al., 2012). Here we chose a parameterization that yields realistic SMBs for Greenland for the historical period (see Section 3). Given the computational advantages of the used coarse resolution version of MPI-ESM in connection with the EBM for long-term simulations, these limitations and differences are an acceptable compromise.

Analyzing the MPI-ESM-CR deglaciation experiments for Greenland, we find that the SMB changes in the beginning of the deglaciation are associated with compensating effects of increasing accumulation and melt. The increase in accumulation dominates the increase in melt until about ~~14 ka BP~~14 ka, as a significant melt is not evident before. After ~~14 ka BP~~ 14 ka the SMB decreases, indicating that this time marks the onset of the deglaciation. The ELA begins to increase significantly earlier, from about ~~19 ka BP~~19 ka, suggesting that the deglaciation of Greenland might have been triggered earlier, likely by the insolation increase that set in before ~~21 ka BP~~21 ka. For Eurasia and North America, the ELA increases continuously from ~~21 ka~~21 ka, supporting such a hypothesis. An onset of the deglaciation over Greenland at around ~~14 ka BP~~ 14 ka is found in reconstructions and has been connected to the Bølling-Allerød warm period, which was associated with a strong AMOC and warm North Atlantic temperatures (e.g., Clark et al., 2002; Weaver et al., 2003). In MPI-ESM-CR, we do not find such warming but instead find an AMOC slowdown at ~~14.6 ka BP~~14.6 ka. This slowdown is caused by a meltwater pulse of more than ~~0.4 Sv~~0.4 Sv, prescribed by the ~~ice sheet~~ ice-sheet reconstructions (meltwater pulse 1A). As this meltwater pulse is associated with ice volume changes mostly in the North Atlantic/Arctic drainage basin in the ~~ice sheet~~ ice-sheet reconstructions, it is assumed that the meltwater enters the North Atlantic and Arctic. This meltwater reduces the AMOC, which is associated with the strong cooling in the North Atlantic realm, in our model. The model does not simulate the strong melting needed for meltwater pulse 1A. After the end of the prescribed melt water peak the AMOC recovers in the model with some overshooting of the AMOC (peaking after ~~200–300 a BP~~200 a BP–300 a BP). This result indicates that although our model does not simulate the Bølling-Allerød warm period as represented in proxy data, the overall progression of the deglaciation is represented reasonably well.

A comparison between ELAs and SMBs derived from MPI-ESM-CR simulations with different ice-sheet reconstructions (Glac1D and Ice6G) as boundary forcing reveals that the results are qualitatively similar (see Fig. A2 to A6), although modeled changes in the AMOC are highly dependent on where the forcing is applied (e.g., Tarasov and Peltier, 2005). The comparison shows that the changes presented here are relatively robust, specifically for changes in the ELA. Exploring the differences in the model response due to prescribed ice-sheet reconstructions is subject to a future study.

The AMOC slowdowns that occur throughout the last deglaciation are associated with significant changes of the ELA and SMB, specifically over Greenland and regionally also for the Eurasian and North American ice sheets. They are associated with cooling over the North Atlantic and a decrease in accumulation and melting in the adjacent regions. While the response in melt is directly affected by temperature changes, accumulation not only directly depends on temperature, affecting the quantitative distribution of snow- and rainfall, but also on other atmospheric properties, e.g., the capability of the atmosphere to hold water, changes in the atmospheric circulation and convection (Trenberth, 2011). The differences in the ELA in response to the AMOC slowdowns over the Laurentide and Eurasian ice sheets further away from the North Atlantic coasts are challenging to interpret for the following reasons. Substantial changes in the ice sheet height and volume cause significant surface warming and enhance melting specifically at the southern margins of the ice sheets (Fig. 7 or 6). Further, other contributing factors are more difficult to separate due to the nature of the experimental design, such as the effect of sea-level changes on the ice sheet margins, feedbacks in response to changes in the sea level, sea ice, and greenhouse gases as the ice sheet height (see e.g. Fyke et al., 2018). In addition, the missing ~~ice sheet~~ ice-sheet dynamics might result in a modified ELA response due to differences in the ~~ice sheet~~ ice-sheet height and configuration (Cronin, 2010). ~~The latter would require the incorporation of~~ Utilizing the SMB data set presented here as forcing for ice-sheet model simulations will allow for an investigation of ice-sheet dynamics during the last deglaciation. In the future, we will utilize the EBM in simulations with an interactive ice sheet model, which is currently employed within the MPI-ESM setup in the scope of the project PalMod (Latif et al., 2016; Ziemen et al., 2019). ~~Utilizing the SMB data set presented here as forcing for ice sheet model simulations will allow for an investigation of ice sheet dynamics.~~

~~A comparison between ELAs and SMBs derived from MPI-ESM-CR simulations with different ice sheet reconstructions (Glac1D and Ice6G) as boundary forcing reveals that the results are qualitatively similar (see Fig. A2 to A6). However, the modeled changes in the AMOC are highly dependent on where the forcing is applied (e.g., Tarasov and Peltier, 2005). The scope of this study is not to evaluate the forcing data sets used here,~~ The setup presented here is an important component of the fully coupled MPI climate–ice-sheet model system. Simulations with the full setup will allow to investigate feedback processes between ice sheets and the other climate components (see e.g. Fyke et al., 2018, for a recent review). It will also allow to investigate processes and test hypotheses arising from the deglaciation simulations for other climates, such as e.g. ~~, the ice volume changes as prescribed by the reconstructions. All reconstructions pose unexplored uncertainties (Kageyama et al., 2017). However, the comparison shows that the changes presented here are relatively robust, specifically for changes in the ELA. Exploring the differences in the model response due to prescribed ice sheet reconstructions is subject to a futurestudy~~the last glacial inception, Marine Isotope Stage 3 as well as the future.

Code and data availability. MPI-ESM is available under the Software License Agreement version 2 after acceptance of a license (https://www.mpimet.mpg.de/en/science/models/license/). The 3-D SMB data set as well as ocean forcing required to conduct ice sheet model experiments for the deglaciation experiments with different ice-sheet reconstructions can be obtained from the DKRZ World Data Center for Climate (WDCC) at https://cera-www.dkrz.de/WDCC/ui/cerasearch/entry?acronym=DKRZ_LTA_989_ds00006 (Glac1D boundary conditions) and https://cera-www.dkrz.de/WDCC/ui/cerasearch/entry?acronym=DKRZ_LTA_989_ds00007 (Ice6G). Additional data sets are available from the corresponding author upon request.

Appendix A: Supplementary Figures

Author contributions. MK, FZ and UM developed the idea for the manuscript. UM, CR and MK advanced the EBM model code and UM adapted MPI-ESM-CR for transient deglaciation simulations. UM performed the deglaciation and MK the millenniums and historical simulations with the MPI-ESM-CR setup. MK conducted the analysis and wrote the manuscript, with contribution to Section 2.1 by CR. CS, MK and FZ prepared the ice-sheet model forcing data. All authors commented and improved the manuscript.

Competing interests. The authors declare that they have no conflict of interest.

Acknowledgements. This project was supported by the German Federal Ministry of Education and Research (BMBF) as a Research for Sustainability initiative (FONA) through the PalMod project under grant no. 01LP1504C, 01LP1502A, 01LP1915 and 01LP1917. Christian Rodehacke has received funding from the European Research Council under the European Community's Seventh Framework Programme (FP7/2007-2013) grant agreement 226520 (COMBINE, EC IP) and (FP7/2007–2013)/ERC grant agreement 610055 as part of the Ice2Ice project. All simulations were performed at the German Climate Computing Center (DKRZ). We also acknowledge the ECMWF for granting access to the ERA-Interim reanalysis. Furthermore, we like to thank Xavier Fettweis and Brice Noël for providing the MAR and RACMO data. We thank Stephan Lorenz for assisting with the setup and Matthew Toohey for providing the volcanic forcing for the last millennium simulations. We also thank Heinrich Widmann for assisting us to store our data at the World Data Center for Climate (WDCC) and the WDCC for hosting our dataset. Additionally, we are grateful to Thomas Kleinen ~~for his~~ and two anonymous reviewers for their helpful comments to improve this manuscript.

References

Abe-Ouchi, A., Segawa, T., and Saito, F. (2007). Climatic conditions for modelling the northern hemisphere ice sheets throughout the ice age cycle. *Climate of the Past*, 3(3):423–438.

Agosta, C., Amory, C., Kittel, C., Orsi, A., Favier, V., Gallée, H., van den Broeke, M. R., Lenaerts, J. T. M., van Wessem, J. M., van de Berg, W. J., and Fettweis, X. (2019). Estimation of the antarctic surface mass balance using the regional climate model mar (1979–2015) and identification of dominant processes. *The Cryosphere*, 13(1):281–296.

Andres, H. J. and Tarasov, L. (2019). Towards understanding potential atmospheric contributions to abrupt climate changes: characterizing changes to the north atlantic eddy-driven jet over the last deglaciation. *Climate of the Past*, 15(4):1621–1646.

Bauer, E. and Ganopolski, A. (2017). Comparison of surface mass balance of ice sheets simulated by positive-degree-day method and energy balance approach. *Climate of the Past*, 13(7):819–832.

Berger, A. and Loutre, M. (1991). Insolation values for the climate of the last 10 million years. *Quaternary Science Reviews*, 10(4):297 – 317.

Bolton, D. (1980). The Computation of Equivalent Potential Temperature. *Monthly Weather Review*, 108(7):1046–1053.

Box, J. E. (2013). Greenland Ice Sheet Mass Balance Reconstruction. Part II: Surface Mass Balance (1840–2010). *Journal of Climate*, 26(18):6974–6989.

Briggs, R. D., Pollard, D., and Tarasov, L. (2014). A data-constrained large ensemble analysis of antarctic evolution since the eemian. *Quaternary Science Reviews*, 103:91 – 115.

Budd, W. and Smith, I. (1981). The growth and retreat of ice sheets in response to orbital radiation changes. International Association of Hydrological Sciences Publication 131 (Symposium at Canberra 1979 — Sea Level, Ice, and Climate Change), 369–409.

Carlson, A. E., Clark, P. U., Haley, B. A., Klinkhammer, G. P., Simmons, K., Brook, E. J., and Meissner, K. J. (2007). Geochemical proxies of north american freshwater routing during the younger dryas cold event. *Proceedings of the National Academy of Sciences*, 104(16):6556–6561.

Chylek, P., Dubey, M. K., and Lesins, G. (2006). Greenland warming of 1920–1930 and 1995–2005. *Geophysical Research Letters*, 33(11).

Clark, P. U., Dyke, A. S., Shakun, J. D., Carlson, A. E., Clark, J., Wohlfarth, B., Mitrovica, J. X., Hostetler, S. W., and McCabe, A. M. (2009). The last glacial maximum. *Science*, 325(5941):710–714.

Clark, P. U., Pisias, N. G., Stocker, T. F., and Weaver, A. J. (2002). The role of the thermohaline circulation in abrupt climate change. *Nature*, 415(6874):863–869.

Clark, P. U., Shakun, J. D., Baker, P. A., Bartlein, P. J., Brewer, S., Brook, E., Carlson, A. E., Cheng, H., Kaufman, D. S., Liu, Z., Marchitto, T. M., Mix, A. C., Morrill, C., Otto-Bliesner, B. L., Pahnke, K., Russell, J. M., Whitlock, C., Adkins, J. F., Blois, J. L., Clark, J., Colman, S. M., Curry, W. B., Flower, B. P., He, F., Johnson, T. C., Lynch-Stieglitz, J., Markgraf, V., McManus, J., Mitrovica, J. X., Moreno, P. I., and Williams, J. W. (2012). Global climate evolution during the last deglaciation. *Proceedings of the National Academy of Sciences*, 109(19):E1134–E1142.

Cox, C. J., Walden, V. P., and Rowe, P. M. (2012). A comparison of the atmospheric conditions at eureka, canada, and barrow, alaska (2006–2008). *Journal of Geophysical Research: Atmospheres*, 117(D12).

Cronin, T. M. (2010). *Millennial Climate Events During Deglaciation*, pages 185–214. Columbia University Press.

Cuffey, K. M. and Paterson, W. (2010). *The Physics of Glaciers*. Oxford, UK: Elsevier Inc., 4 edition.

Dee, D. P., Uppala, S. M., Simmons, A. J., Berrisford, P., Poli, P., Kobayashi, S., Andrae, U., Balmaseda, M. A., Balsamo, G., Bauer, P., Bechtold, P., Beljaars, A. C. M., van de Berg, L., Bidlot, J., Bormann, N., Delsol, C., Dragani, R., Fuentes, M., Geer, A. J., Haimberger, L., Healy, S. B., Hersbach, H., HÃ^{3}lm, E. V., Isaksen, L., KÃ¥llberg, P., KÃ¶hler, M., Matricardi, M., McNally, A. P., Monge-Sanz, B. M., Morcrette, J.-J., Park, B.-K., Peubey, C., de Rosnay, P., Tavolato, C., ThÃ©paut, J.-N., and Vitart, F. (2011). The era-interim reanalysis: configuration and performance of the data assimilation system. *Quarterly Journal of the Royal Meteorological Society*, 137(656):553–597.

Ettema, J., van den Broeke, M. R., van Meijgaard, E., van de Berg, W. J., Bamber, J. L., Box, J. E., and Bales, R. C. (2009). Higher surface mass balance of the greenland ice sheet revealed by high-resolution climate modeling. *Geophysical Research Letters*, 36(12).

Fettweis, X. (2007). Reconstruction of the 1979–2006 greenland ice sheet surface mass balance using the regional climate model mar. *The Cryosphere*, 1(1):21–40.

Fettweis, X., Box, J. E., Agosta, C., Amory, C., Kittel, C., Lang, C., van As, D., Machguth, H., and Gallée, H. (2017). Reconstructions of the 1900–2015 greenland ice sheet surface mass balance using the regional climate mar model. *The Cryosphere*, 11(2):1015–1033.

Fettweis, X., Franco, B., Tedesco, M., van Angelen, J. H., Lenaerts, J. T. M., van den Broeke, M. R., and Gallée, H. (2013). Estimating the greenland ice sheet surface mass balance contribution to future sea level rise using the regional atmospheric climate model mar. *The Cryosphere*, 7(2):469–489.

Fettweis, X., Hanna, E., Gallée, H., Huybrechts, P., and Erpicum, M. (2008). Estimation of the greenland ice sheet surface mass balance for the 20th and 21st centuries. *The Cryosphere*, 2(2):117–129.

Fettweis, X., Hofer, S., Krebs-Kanzow, U., Amory, C., Aoki, T., Berends, C. J., Born, A., Box, J. E., Delhasse, A., Fujita, K., Gierz, P., Goelzer, H., Hanna, E., Hashimoto, A., Huybrechts, P., Kapsch, M.-L., King, M. D., Kittel, C., Lang, C., Langen, P. L., Lenaerts, J. T. M., Liston, G. E., Lohmann, G., Mernild, S. H., Mikolajewicz, U., Modali, K., Mottram, R. H., Niwano, M., Noël, B., Ryan, J. C., Smith, A., Streffing, J., Tedesco, M., van de Berg, W. J., van den Broeke, M., van de Wal, R. S. W., van Kampenhout, L., Wilton, D., Wouters, B., Ziemen, F., and Zolles, T. (2020). Grsmbmip: intercomparison of the modelled 1980–2012 surface mass balance over the greenland ice sheet. *The Cryosphere*, 14(11):3935–3958.

Fukusako, S. (1990). Thermophysical properties of ice, snow, and sea ice. *International Journal of Thermophysics*, 11(2):353–372.

Fyke, J., Sergienko, O., Löfverström, M., Price, S., and Lenaerts, J. T. M. (2018). An overview of interactions and feedbacks between ice sheets and the earth system. *Reviews of Geophysics*, 56(2):361–408.

Greuell, W. and Konzelmann, T. (1994a). Numerical modelling of the energy balance and the englacial temperature of the greenland ice sheet. calculations for the eth-camp location (west greenland, 1155 m a.s.l.). *Global and Planetary Change*, 9(1):91 – 114. Greenland ice margin experiment (GIMEx).

Greuell, W. and Konzelmann, T. (1994b). Numerical modelling of the energy balance and the englacial temperature of the greenland ice sheet. calculations for the eth-camp location (west greenland, 1155 m a.s.l.). *Global and Planetary Change*, 9(1):91 – 114. Greenland ice margin experiment (GIMEx).

Hanna, E., Huybrechts, P., Cappelen, J., Steffen, K., Bales, R. C., Burgess, E., McConnell, J. R., Peder Steffensen, J., Van den Broeke, M., Wake, L., Bigg, G., Griffiths, M., and Savas, D. (2011). Greenland ice sheet surface mass balance 1870 to 2010 based on twentieth century reanalysis, and links with global climate forcing. *Journal of Geophysical Research: Atmospheres*, 116(D24).

Heinrich, H. (1988). Origin and consequences of cyclic ice rafting in the northeast atlantic ocean during the past 130,000 years. *Quaternary Research*, 29(2):142 – 152.

Horton, B. P., Rahmstorf, S., Engelhart, S. E., and Kemp, A. C. (2014). Expert assessment of sea-level rise by ad 2100 and ad 2300. *Quaternary Science Reviews*, 84:1 – 6.

Jungclaus, J. H., Lorenz, S. J., Timmreck, C., Reick, C. H., Brovkin, V., Six, K., Segschneider, J., Giorgetta, M. A., Crowley, T. J., Pongratz, J., Krivova, N. A., Vieira, L. E., Solanki, S. K., Klocke, D., Botzet, M., Esch, M., Gayler, V., Haak, H., Raddatz, T. J., Roeckner, E., Schnur, R., Widmann, H., Claussen, M., Stevens, B., and Marotzke, J. (2010). Climate and carbon-cycle variability over the last millennium. *Climate of the Past*, 6(5):723–737.

Kageyama, M., Albani, S., Braconnot, P., Harrison, S. P., Hopcroft, P. O., Ivanovic, R. F., Lambert, F., Marti, O., Peltier, W. R., Peterschmitt, J.-Y., Roche, D. M., Tarasov, L., Zhang, X., Brady, E. C., Haywood, A. M., LeGrande, A. N., Lunt, D. J., Mahowald, N. M., Mikolajewicz, U., Nisancioglu, K. H., Otto-Bliesner, B. L., Renssen, H., Tomas, R. A., Zhang, Q., Abe-Ouchi, A., Bartlein, P. J., Cao, J., Li, Q., Lohmann, G., Ohgaito, R., Shi, X., Volodin, E., Yoshida, K., Zhang, X., and Zheng, W. (2017). The pmip4 contribution to cmip6 – part 4: Scientific objectives and experimental design of the pmip4-cmip6 last glacial maximum experiments and pmip4 sensitivity experiments. *Geoscientific Model Development*, 10(11):4035–4055.

Kageyama, M., Harrison, S. P., Kapsch, M.-L., Löfverström, M., Lora, J. M., Mikolajewicz, U., Sherriff-Tadano, S., Vadsaria, T., Abe-Ouchi, A., Bouttes, N., Chandan, D., LeGrande, A. N., Lhardy, F., Lohmann, G., Morozova, P. A., Ohgaito, R., Peltier, W. R., Quiquet, A., Roche, D. M., Shi, X., Schmittner, A., Tierney, J. E., and Volodin, E. (2020). The pmip4-cmip6 last glacial maximum experiments: preliminary results and comparison with the pmip3-cmip5 simulations. *Climate of the Past Discussions*, 2020:1–37.

Keigwin, L. D. and Lehman, S. J. (1994). Deep circulation change linked to heinrich event 1 and younger dryas in a middepth north atlantic core. *Paleoceanography*, 9(2):185–194.

Khan, S. A., Aschwanden, A., Bjørk, A. A., Wahr, J., Kjeldsen, K. K., and Kjær, K. H. (2015). Greenland ice sheet mass balance: a review. *Reports on Progress in Physics*, 78(4):046801.

Klockmann, M., Mikolajewicz, U., and Marotzke, J. (2016). The effect of greenhouse gas concentrations and ice sheets on the glacial amoc in a coupled climate model. *Climate of the Past*, 12(9):1829–1846.

Klok, E. J. and Oerlemans, J. (2004). Modelled climate sensitivity of the mass balance of morteratschgletscher and its dependence on albedo parameterization. *International Journal of Climatology*, 24(2):231–245.

Köhler, P., Nehrbass-Ahles, C., Schmitt, J., Stocker, T. F., and Fischer, H. (2017). A 156 kyr smoothed history of the atmospheric greenhouse gases co_2, ch_4, and n_2o and their radiative forcing. *Earth System Science Data*, 9(1):363–387.

Latif, M., Claussen, M., Schulz, M., and Brücher, T. (2016). Comprehensive earth system models of the last glacial cycle. *EOS*, 97.

Le clec'h, S., Charbit, S., Quiquet, A., Fettweis, X., Dumas, C., Kageyama, M., Wyard, C., and Ritz, C. (2019). Assessment of the greenland ice sheet–atmosphere feedbacks for the next century with a regional atmospheric model coupled to an ice sheet model. *The Cryosphere*, 13(1):373–395.

Lenaerts, J. T. M., van den Broeke, M. R., van de Berg, W. J., van Meijgaard, E., and Kuipers Munneke, P. (2012). A new, high-resolution surface mass balance map of antarctica (1979–2010) based on regional atmospheric climate modeling. *Geophysical Research Letters*, 39(4).

Lenaerts, J. T. M., Van Tricht, K., Lhermitte, S., and L'Ecuyer, T. S. (2017). Polar clouds and radiation in satellite observations, reanalyses, and climate models. *Geophysical Research Letters*, 44(7):3355–3364.

Lipscomb, W. H., Fyke, J. G., Vizcaíno, M., Sacks, W. J., Wolfe, J., Vertenstein, M., Craig, A., Kluzek, E., and Lawrence, D. M. (2013). Implementation and Initial Evaluation of the Glimmer Community Ice Sheet Model in the Community Earth System Model. *Journal of Climate*, 26(19):7352–7371.

Liston, G. E., Bruland, O., Winther, J.-G., ElvehÃžy, H., and Sand, K. (1999). Meltwater production in antarctic blue-ice areas: sensitivity to changes in atmospheric forcing. *Polar Research*, 18(2):283–290.

Löfverström, M. (2020). A dynamic link between high-intensity precipitation events in southwestern north america and europe at the last glacial maximum. *Earth and Planetary Science Letters*, 534:116081.

Löfverström, M. and Lora, J. M. (2017). Abrupt regime shifts in the north atlantic atmospheric circulation over the last deglaciation. *Geophysical Research Letters*, 44(15):8047–8055.

Marsland, S., Haak, H., Jungclaus, J., Latif, M., and RÃ¶ske, F. (2003). The max-planck-institute global ocean/sea ice model with orthogonal curvilinear coordinates. *Ocean Modelling*, 5(2):91 – 127.

Marty, C., Philipona, R., Fröhlich, C., and Ohmura, A. (2002). Altitude dependence of surface radiation fluxes and cloud forcing in the alps: results from the alpine surface radiation budget network. *Theoretical and Applied Climatology*, 72(3):137–155.

Mauritsen, T., Bader, J., Becker, T., Behrens, J., Bittner, M., Brokopf, R., Brovkin, V., Claussen, M., Crueger, T., Esch, M., Fast, I., Fiedler, S., Fläschner, D., Gayler, V., Giorgetta, M., Goll, D. S., Haak, H., Hagemann, S., Hedemann, C., Hohenegger, C., Ilyina, T., Jahns, T., Jimenez-de-la Cuesta, D., Jungclaus, J., Kleinen, T., Kloster, S., Kracher, D., Kinne, S., Kleberg, D., Lasslop, G., Kornblueh, L., Marotzke, J., Matei, D., Meraner, K., Mikolajewicz, U., Modali, K., Möbis, B., Müller, W. A., Nabel, J. E. M. S., Nam, C. C. W., Notz, D., Nyawira, S.-S., Paulsen, H., Peters, K., Pincus, R., Pohlmann, H., Pongratz, J., Popp, M., Raddatz, T. J., Rast, S., Redler, R., Reick, C. H., Rohrschneider, T., Schemann, V., Schmidt, H., Schnur, R., Schulzweida, U., Six, K. D., Stein, L., Stemmler, I., Stevens, B., von Storch, J.-S., Tian, F., Voigt, A., Vrese, P., Wieners, K.-H., Wilkenskjeld, S., Winkler, A., and Roeckner, E. (2019). Developments in the mpi-m earth system model version 1.2 (mpi-esm1.2) and its response to increasing co2. *Journal of Advances in Modeling Earth Systems*, 11(4):998–1038.

McManus, J. F., Francois, R., Gherardi, J. M., Keigwin, L. D., and Brown-Leger, S. (2004). Collapse and rapid resumption of atlantic meridional circulation linked to deglacial climate changes. *Nature*, 428(6985):834–837.

Meccia, V. L. and Mikolajewicz, U. (2018). Interactive ocean bathymetry and coastlines for simulating the last deglaciation with the max planck institute earth system model (mpi-esm-v1.2). *Geoscientific Model Development*, 11(11):4677–4692.

Mikolajewicz, U., Gröger, M., Maier-Reimer, E., Schurgers, G., Vizcaíno, M., and Winguth, A. M. E. (2007). Long-term effects of anthropogenic co2 emissions simulated with a complex earth system model. *Climate Dynamics*, 28(6):599–633.

Mikolajewicz, U., Ziemen, F., Cioni, G., Claussen, M., Fraedrich, K., Heidkamp, M., Hohenegger, C., Jimenez de la Cuesta, D., Kapsch, M.-L., Lemburg, A., Mauritsen, T., Meraner, K., Röber, N., Schmidt, H., Six, K. D., Stemmler, I., Tamarin-Brodsky, T., Winkler, A., Zhu, X., and Stevens, B. (2018). The climate of a retrograde rotating earth. *Earth System Dynamics*, 9(4):1191–1215.

Miller, N. B., Shupe, M. D., Lenaerts, J. T. M., Kay, J. E., de Boer, G., and Bennartz, R. (2018). Process-based model evaluation using surface energy budget observations in central greenland. *Journal of Geophysical Research: Atmospheres*, 123(10):4777–4796.

Noël, B., van de Berg, W. J., Lhermitte, S., and van den Broeke, M. R. (2019). Rapid ablation zone expansion amplifies north greenland mass loss. *Science Advances*, 5(9).

Noël, B., van de Berg, W. J., van Wessem, J. M., van Meijgaard, E., van As, D., Lenaerts, J. T. M., Lhermitte, S., Kuipers Munneke, P., Smeets, C. J. P. P., van Ulft, L. H., van de Wal, R. S. W., and van den Broeke, M. R. (2018). Modelling the climate and surface mass balance of polar ice sheets using racmo2 – part 1: Greenland (1958–2016). *The Cryosphere*, 12(3):811–831.

Nowicki, S. M. J., Payne, A., Larour, E., Seroussi, H., Goelzer, H., Lipscomb, W., Gregory, J., Abe-Ouchi, A., and Shepherd, A. (2016). Ice sheet model intercomparison project (ismip6) contribution to cmip6. *Geoscientific Model Development*, 9(12):4521–4545.

Oerlemans, J. and Knap, W. H. (1998). A 1 year record of global radiation and albedo in the ablation zone of morteratschgletscher, switzerland. *Journal of Glaciology*, 44(147):231–238.

Patton, H., Hubbard, A., Andreassen, K., Auriac, A., Whitehouse, P. L., Stroeven, A. P., Shackleton, C., Winsborrow, M., Heyman, J., and Hall, A. M. (2017). Deglaciation of the eurasian ice sheet complex. *Quaternary Science Reviews*, 169:148 – 172.

Peltier, W. R., Argus, D. F., and Drummond, R. (2015). Space geodesy constrains ice age terminal deglaciation: The global ice-6g_c (vm5a) model. *Journal of Geophysical Research: Solid Earth*, 120(1):450–487.

Pfeffer, W. T., Meier, M. F., and Illangasekare, T. H. (1991). Retention of greenland runoff by refreezing: Implications for projected future sea level change. *Journal of Geophysical Research: Oceans*, 96(C12):22117–22124.

Raddatz, T. J., Reick, C. H., Knorr, W., Kattge, J., Roeckner, E., Schnur, R., Schnitzler, K. G., Wetzel, P., and Jungclaus, J. (2007). Will the tropical land biosphere dominate the climate–carbon cycle feedback during the twenty-first century? *Climate Dynamics*, 29(6):565–574.

Riddick, T., Brovkin, V., Hagemann, S., and Mikolajewicz, U. (2018). Dynamic hydrological discharge modelling for coupled climate model simulations of the last glacial cycle: the mpi-dynamichd model version 3.0. *Geoscientific Model Development*, 11(10):4291–4316.

Schmidt, G. A., Jungclaus, J. H., Ammann, C. M., Bard, E., Braconnot, P., Crowley, T. J., Delaygue, G., Joos, F., Krivova, N. A., Muscheler, R., Otto-Bliesner, B. L., Pongratz, J., Shindell, D. T., Solanki, S. K., Steinhilber, F., and Vieira, L. E. A. (2012). Climate forcing reconstructions for use in pmip simulations of the last millennium (v1.1). *Geoscientific Model Development*, 5(1):185–191.

Schwerdtfeger, P. (1963). *Theoretical Derivation of the Thermal Conductivity and Diffusivity of Snow*, volume 61. IAHS Press - Intern. Assoc. Hydrological Science, Seattle, Washington, USA.

Stanford, J., Rohling, E., Bacon, S., Roberts, A., Grousset, F., and Bolshaw, M. (2011). A new concept for the paleoceanographic evolution of heinrich event 1 in the north atlantic. *Quaternary Science Reviews*, 30(9):1047 – 1066.

Stengel, M., Schlundt, C., Stapelberg, S., Sus, O., Eliasson, S., Willén, U., and Meirink, J. F. (2018). Comparing era-interim clouds with satellite observations using a simplified satellite simulator. *Atmospheric Chemistry and Physics*, 18(23):17601–17614.

Stevens, B., Giorgetta, M., Esch, M., Mauritsen, T., Crueger, T., Rast, S., Salzmann, M., Schmidt, H., Bader, J., Block, K., Brokopf, R., Fast, I., Kinne, S., Kornblueh, L., Lohmann, U., Pincus, R., Reichler, T., and Roeckner, E. (2013). Atmospheric component of the mpi-m earth system model: Echam6. *Journal of Advances in Modeling Earth Systems*, 5(2):146–172.

Suzuki, K., Kubota, J., Zhang, Y., Kadota, T., Ohata, T., and Vuglinksy, V. (2006). Snow ablation in an open field and larch forest of the southern mountainous region of eastern siberia. *Hydrological Sciences Journal*, 51(3):465–480.

Tarasov, L., Dyke, A. S., Neal, R. M., and Peltier, W. (2012). A data-calibrated distribution of deglacial chronologies for the north american ice complex from glaciological modeling. *Earth and Planetary Science Letters*, 315-316:30 – 40. Sea Level and Ice Sheet Evolution: A PALSEA Special Edition.

Tarasov, L. and Peltier, W. R. (2005). Arctic freshwater forcing of the younger dryas cold reversal. *Nature*, 435(7042):662–665.

Tarasov, L. and Richard Peltier, W. (2002). Greenland glacial history and local geodynamic consequences. *Geophysical Journal International*, 150(1):198–229.

Trenberth, K. E. (2011). Changes in precipitation with climate change. *Climate Research*, 47(1-2):123–138.

van Angelen, J. H., Lenaerts, J. T. M., Lhermitte, S., Fettweis, X., Kuipers Munneke, P., van den Broeke, M. R., van Meijgaard, E., and Smeets, C. J. P. P. (2012). Sensitivity of greenland ice sheet surface mass balance to surface albedo parameterization: a study with a regional climate model. *The Cryosphere*, 6(5):1175–1186.

van den Broeke, M., Bamber, J., Ettema, J., Rignot, E., Schrama, E., van de Berg, W. J., van Meijgaard, E., Velicogna, I., and Wouters, B. (2009). Partitioning recent greenland mass loss. *Science*, 326(5955):984–986.

van Kampenhout, L., Lenaerts, J. T. M., Lipscomb, W. H., Sacks, W. J., Lawrence, D. M., Slater, A. G., and van den Broeke, M. R. (2017). Improving the representation of polar snow and firn in the community earth system model. *Journal of Advances in Modeling Earth Systems*, 9(7):2583–2600.

van Kampenhout, L., Rhoades, A. M., Herrington, A. R., Zarzycki, C. M., Lenaerts, J. T. M., Sacks, W. J., and van den Broeke, M. R. (2019). Regional grid refinement in an earth system model: impacts on the simulated greenland surface mass balance. *The Cryosphere*, 13(6):1547–1564.

van Wessem, J. M., van de Berg, W. J., Noël, B. P. Y., van Meijgaard, E., Amory, C., Birnbaum, G., Jakobs, C. L., Krüger, K., Lenaerts, J. T. M., Lhermitte, S., Ligtenberg, S. R. M., Medley, B., Reijmer, C. H., van Tricht, K., Trusel, L. D., van Ulft, L. H., Wouters, B., Wuite, J., and van den Broeke, M. R. (2018). Modelling the climate and surface mass balance of polar ice sheets using racmo2 – part 2: Antarctica (1979–2016). *The Cryosphere*, 12(4):1479–1498.

Vidal, L., Labeyrie, L., Cortijo, E., Arnold, M., Duplessy, J., Michel, E., BecquÃ©, S., and van Weering, T. (1997). Evidence for changes in the north atlantic deep water linked to meltwater surges during the heinrich events. *Earth and Planetary Science Letters*, 146(1):13 – 27.

Vizcaíno, M. (2014). Ice sheets as interactive components of earth system models: progress and challenges. *WIREs Climate Change*, 5(4):557–568.

Vizcaíno, M., Lipscomb, W. H., Sacks, W. J., van Angelen, J. H., Wouters, B., and van den Broeke, M. R. (2013). Greenland Surface Mass Balance as Simulated by the Community Earth System Model. Part I: Model Evaluation and 1850–2005 Results. *Journal of Climate*, 26(20):7793–7812.

Vizcaíno, M., Mikolajewicz, U., Gröger, M., Maier-Reimer, E., Schurgers, G., and Winguth, A. M. E. (2008). Long-term ice sheet–climate interactions under anthropogenic greenhouse forcing simulated with a complex earth system model. *Climate Dynamics*, 31(6):665–690.

Vizcaíno, M., Mikolajewicz, U., Jungclaus, J., and Schurgers, G. (2010). Climate modification by future ice sheet changes and consequences for ice sheet mass balance. *Climate Dynamics*, 34(2):301–324.

Vizcaíno, M., Mikolajewicz, U., Ziemen, F., Rodehacke, C. B., Greve, R., and van den Broeke, M. R. (2015). Coupled simulations of greenland ice sheet and climate change up to a.d. 2300. *Geophysical Research Letters*, 42(10):3927–3935.

Weaver, A. J., Saenko, O. A., Clark, P. U., and Mitrovica, J. X. (2003). Meltwater pulse 1a from antarctica as a trigger of the bølling-allerød warm interval. *Science*, 299(5613):1709–1713.

Wieners, K.-H., Giorgetta, M., Jungclaus, J., Reick, C., Esch, M., Bittner, M., Legutke, S., Schupfner, M., Wachsmann, F., Gayler, V., Haak, H., de Vrese, P., Raddatz, T., Mauritsen, T., von Storch, J.-S., Behrens, J., Brovkin, V., Claussen, M., Crueger, T., Fast, I., Fiedler, S., Hagemann, S., Hohenegger, C., Jahns, T., Kloster, S., Kinne, S., Lasslop, G., Kornblueh, L., Marotzke, J., Matei, D., Meraner, K., Mikolajewicz, U., Modali, K., Müller, W., Nabel, J., Notz, D., Peters, K., Pincus, R., Pohlmann, H., Pongratz, J., Rast, S., Schmidt, H., Schnur, R., Schulzweida, U., Six, K., Stevens, B., Voigt, A., and Roeckner, E. (2019). Mpi-m mpi-esm1.2-lr model output prepared for cmip6 cmip historical.

Wild, M., Ohmura, A., Gilgen, H., and Roeckner, E. (1995). Regional climate simulation with a high resolution gcm: surface radiative fluxes. *Climate Dynamics*, 11(8):469–486.

Yang, K., Koike, T., Stackhouse, P., Mikovitz, C., and Cox, S. J. (2006). An assessment of satellite surface radiation products for highlands with tibet instrumental data. *Geophysical Research Letters*, 33(22).

Yen, Y. (1981). *Review of thermal properties of snow, ice and sea ice*. CRREL report. U.S. Army, Corps of Engineers, Cold Regions Research and Engineering Laboratory.

Ziemen, F. A., Kapsch, M.-L., Klockmann, M., and Mikolajewicz, U. (2019). Heinrich events show two-stage climate response in transient glacial simulations. *Climate of the Past*, 15(1):153–168.

Zygmuntowska, M., Mauritsen, T., Quaas, J., and Kaleschke, L. (2012). Arctic clouds and surface radiation – a critical comparison of satellite retrievals and the era-interim reanalysis. *Atmospheric Chemistry and Physics*, 12(14):6667–6677.

Table 1. List of constants used in the albedo scheme as part of the EBM. Please see Section 2.1 for further details.

Description	Symbol	Value/Comment
Fresh fallen snow	α_{frsnow}	0.92
Firn	α_{firn}	0.72
Snow layer	$\alpha_{snow}(t)$	between α_{frsnow} and α_{firn}; Equation 1
Ice albedo	α_{ice}	0.70
Final albedo of snow	$\alpha_{surface}(t, d_{snow})$	between α_{frsnow} and α_{ice}; Equation 2
Time scale of snow aging	$\hat{\tau_a}$	1/30 day^{-1}
Time scale for aging of refrozen snow and ice	$\hat{\tau_a r}$	1/45 day^{-1}
Depth scale of snow layer thickness	$\hat{d}$	0.0024 m^{-1}; Equation 2
Melted snow/ice	$\alpha_{snow-/icemelt}$	0.55
Refrozen snow	$\alpha_{snowrefrz}$	0.67
Refrozen ice	$\alpha_{icerefrz}$	0.55
Background albedo below snow layer	α_{bg}	for snow aging in Equation 1; defined in Equation 3, where $\alpha_{bg} \leq \alpha_{ice}$
Density dependence of background albedo parameter, factor	q_1	$-4\,10^{-4}\,\text{m}^3\,\text{kg}^{-1}$
Density dependence of background albedo parameter, offset 1	q_2	0.95
Background albedo below refrozen layer	α_{bg}	$\alpha_{bg} = \alpha_{ice}$ for snow aging, Equation 1

Table 2. Simulations performed, as described in Section 2.3. For the deglaciation experiments the topography and ice sheets are taken from reconstructions and change throughout the simulation. For the historical and last millennium simulations those fields remain constant through time.

Period	Experiment Name	Topography/~~Ice Sheet~~ Ice-Sheet Mask	Spin-up
Deglaciation	MPI-ESM-CR	Glac1D (transient)	26 ~~kas BP~~ kyr steady state
(26k–0 ka BP)	MPI-ESM-CR$_{\mathrm{Ice6G}}$	Ice6G (transient)	26 ~~kas BP~~ kyr steady state
Historical	MPI-ESM-CR	Glac1D (950 a BP)	Last millennium simulation
(1850–2010)	MPI-ESM-CR$_{\mathrm{Ice6G}}$	Ice6G (950 a BP)	Last millennium simulation
	MPI-ESM-LR*	CMIP6	Preindustrial steady state

* This simulation contributed to CMIP6 (see Section 2.3).

Table 3. Average and standard deviation of the annual SMB simulated with MAR and the EBM forced with ERA-Interim and a historical MPI-ESM simulation for the years 1980–2010. The annual SMB values are interpolated onto the ~~ISMIP~~ ISMIP6 ice sheet topography (see Section ~~??~~2.3), except for RACMO*. The standard deviation reflects the inter-annual variability. Units are in GT a^{-1}. Accumulation is calculated as residual of the SMB and melt.

Model	SMB	Melt	Accumulation
MAR	340±122	-548	888
RACMO*	367±108	-540	907
$\mathrm{EBM}_{\mathrm{ERAI}}$	344±140	-288	632
$\mathrm{EBM}_{\mathrm{MPI-ESM-LR}}$	351±83	-311	663
$\mathrm{EBM}_{\mathrm{MPI-ESM-CR\ (Glac1D)}}$	275±107	-495	770
$\mathrm{EBM}_{\mathrm{MPI-ESM-CR\ (Ice6G)}}$	307±71	-440	747

* RACMO data are provided on a slightly different topography with 1 km horizontal resolution (see Noël et al., 2019, for details); the impact of the underlying topography on the SMB values is expected to be small.

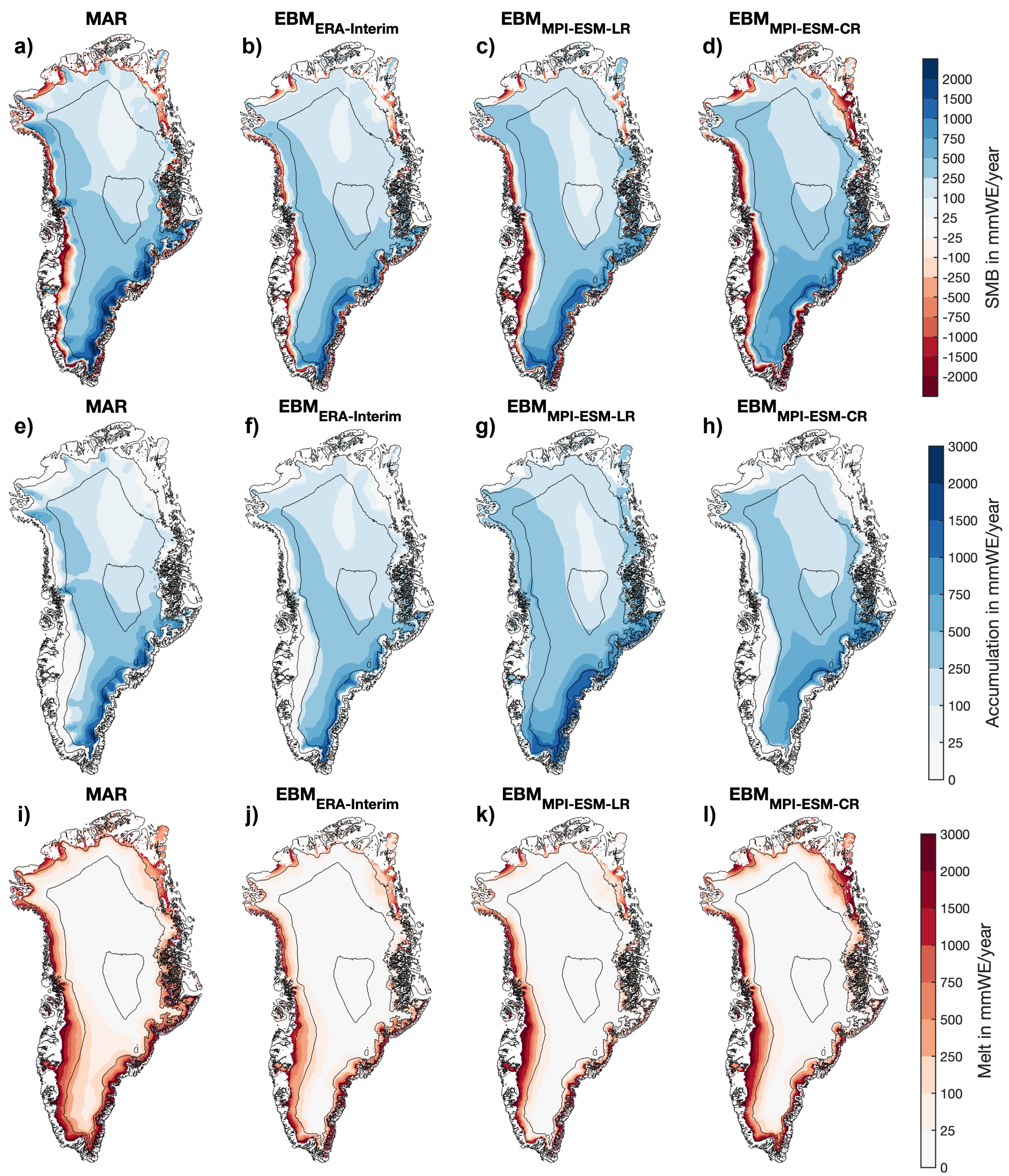

Figure 1. ~~SMB~~ (~~top~~a-d) SMB, ~~accumulation~~ (~~middle~~e-h) accumulation and ~~melt~~ (~~bottom~~i-l) melt from ~~MAR~~ (~~left~~a,e,f) MAR and EBM simulations forced with ~~ERA-Interim~~ (~~center~~b,~~left~~f,j) ERA-Interim, ~~MPI-ESM-LR~~ (~~center~~c,~~right~~g,k) MPI-ESM-LR and ~~MPI-ESM-CR~~ (~~right~~d,h,l) MPI-ESM-CR for historical climate conditions. The values are averaged over 1980–2010. All variables are interpolated on the ISMIP6 topography and shown only for glaciated points. Note that accumulation is obtained as residual of SMB minus melt, as MAR does not provide accumulation as direct output variable. Hence, the contour where accumulation transitions from positive values to zero represents the equilibrium altitude line (ELA). Black contours mark surface elevation at 1000, 2000 and 3000 m.

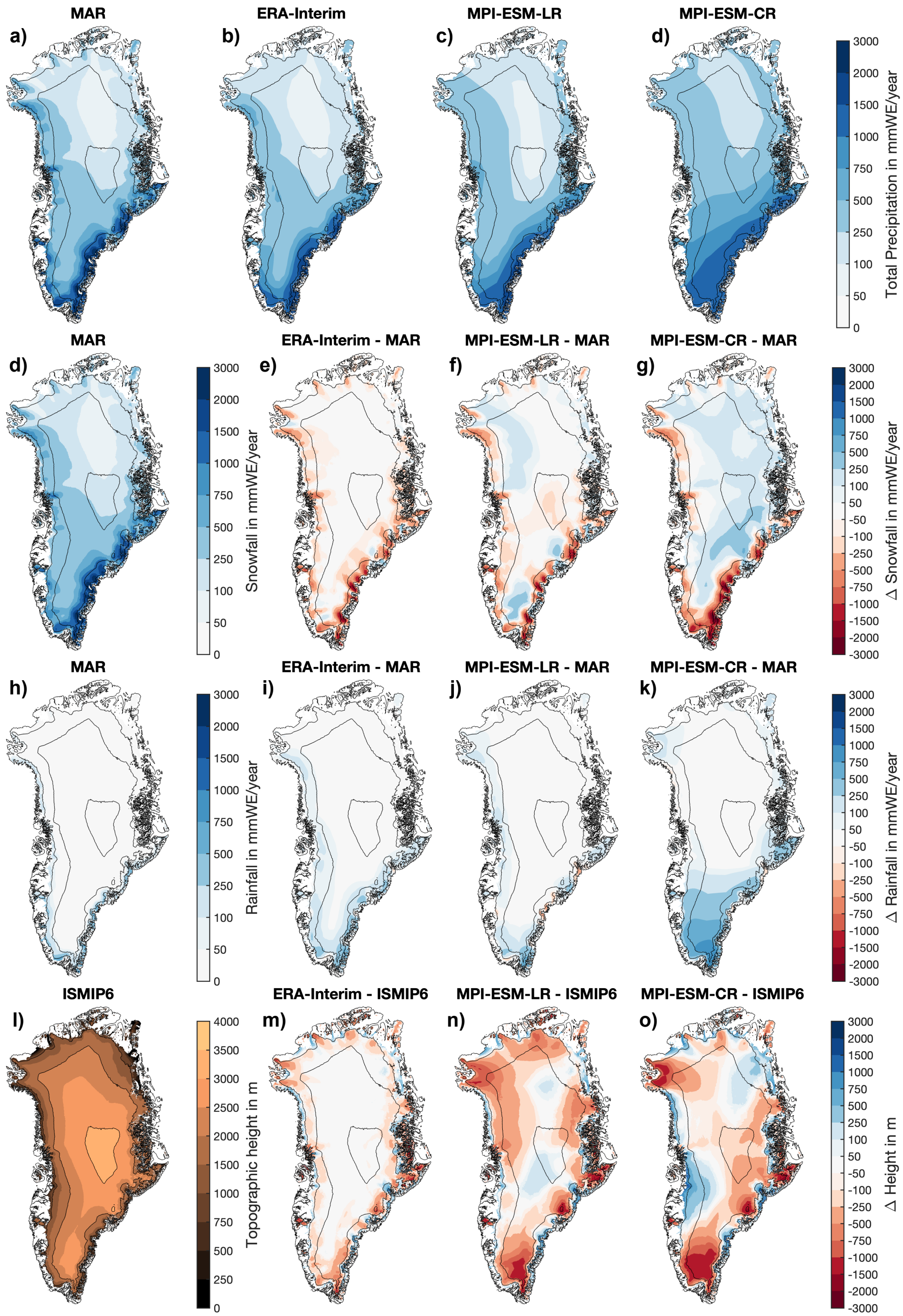

Figure 2. ~~Total Precipitation~~ (~~top~~a-d) Total Precipitation as simulated by ~~MAR~~ (~~left~~a) MAR, ~~ERA-Interim~~ (~~center, left~~b) ERA-Interim, ~~MPI-ESM-LR~~ (~~center, right~~c) MPI-ESM-LR and ~~MPI-ESM-CR~~ (~~right~~d) MPI-ESM-CR for 1980–2010. ~~Snowfall~~ (~~top, middle~~e-h) Snowfall and ~~rainfall~~ (~~bottom, middle~~i-l) rainfall in ~~MAR~~ (~~left~~e,i) MAR and differences between ~~ERA-Interim~~ (~~center~~f,~~left~~j) ERA-Interim, ~~MPI-ESM-LR~~ (~~center~~g,~~right~~k) MPI-ESM-LR and ~~MPI-ESM-CR~~ (~~right~~h,l) MPI-ESM-CR and MAR. ~~Topography~~ (~~bottom~~m-p) Topography from ~~ISMIP6~~ (~~left~~m) ISMIP6 and the differences in topography between ISMIP6 and ~~ERA-Interim~~ (~~center, left~~n) ERA-Interim, ~~MPI-ESM-CR~~ (~~center, right~~o) MPI-ESM-CR and ~~MPI-ESM-LR~~ (~~right~~p) MPI-ESM-LR. Note, that the values are bi-linearly interpolated onto the ISMIP6 topography from the original model data, not the downscaled values. Black contours mark surface elevation at 1000, 2000 and 3000 m.

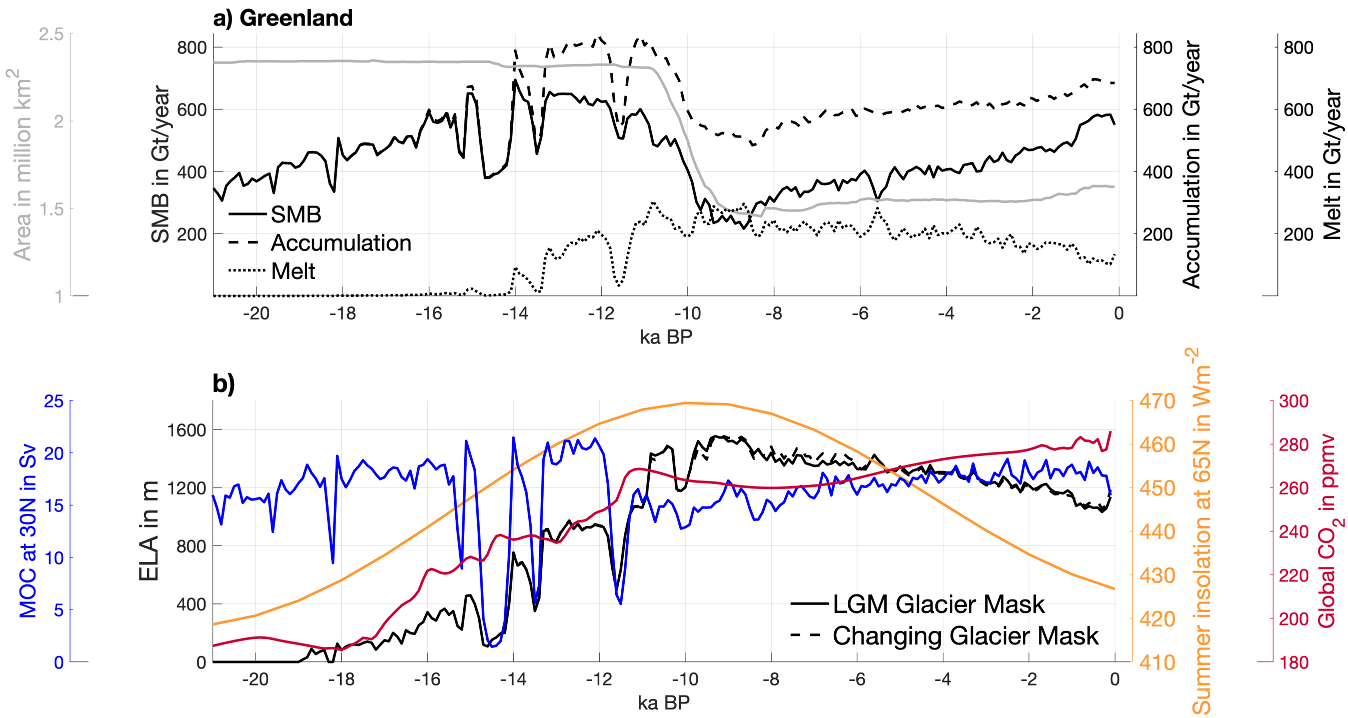

Figure 3. (a) Greenland SMB, accumulation, melt, ice sheet area and (b) Equilibrium Line Altitude (ELA), Meridional Overturning Circulation (MOC) for the $EBM_{MPI-ESM-CR}$ experiment, together with summer insolation at 65°N and CO_2 concentration throughout the last deglaciation (21 ka to 0 ka~~BP~~). Here 0 ka ~~BP~~ refers to the year 1950. SMB, accumulation, melt and ELA (dashed) are integrated over the glacial mask of each individual 100-year time slice. Additionally, the ELA (solid) is integrated over the 21 ka ~~BP ice sheet~~ ice-sheet mask, in order to investigate differences due to the ice-sheet mask. The MOC is the overturning strength at 30.5°N at a depth of 1023 m as in Klockmann et al. (2016). The CO_2 concentration is taken from Köhler et al. (2017) and the summer insolation from Berger and Loutre (1991).

.

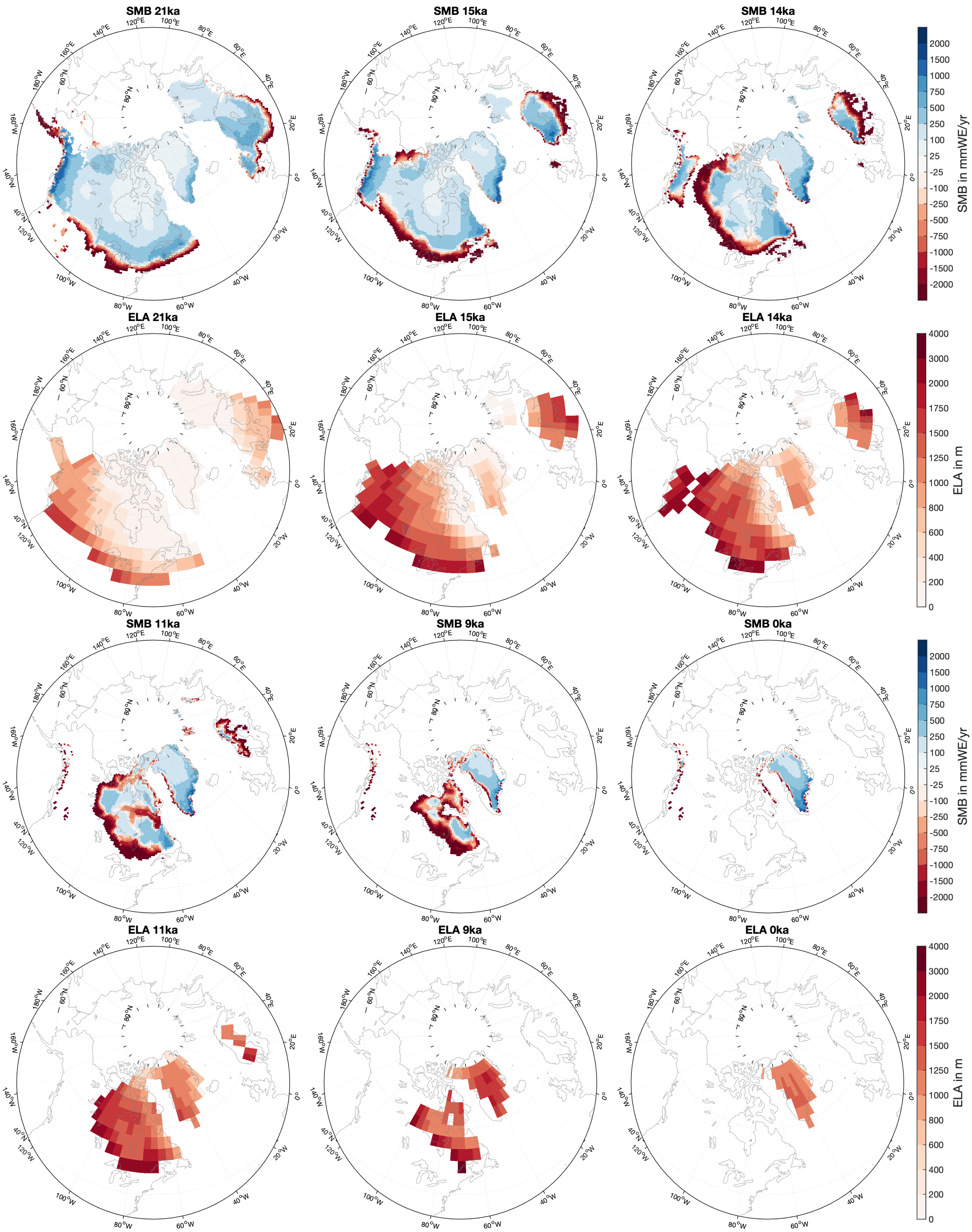

Figure 4. SMB and ELA for selected time slices (21 ka, 15 ka, 14 ka, 11 ka, 9 ka and 0 ka~~BP~~). Shown are 100-year means. The SMB is interpolated on the Glac1D topography for each individual time slice ~~,~~ and masked with the Glac1D glacier mask. The ELA, defined as elevation where the SMB equals zero, is ~~shown~~ calculated for each grid point on the native MPI-ESM-CR model grid from the 3-D SMB (see Sections 2.1 and 2.3). ~~Note that~~ The ELA is masked with the ~~different~~ glacier ~~masks are a result of~~ mask used in the ~~different resolution~~MPI-ESM-CR simulations.

.

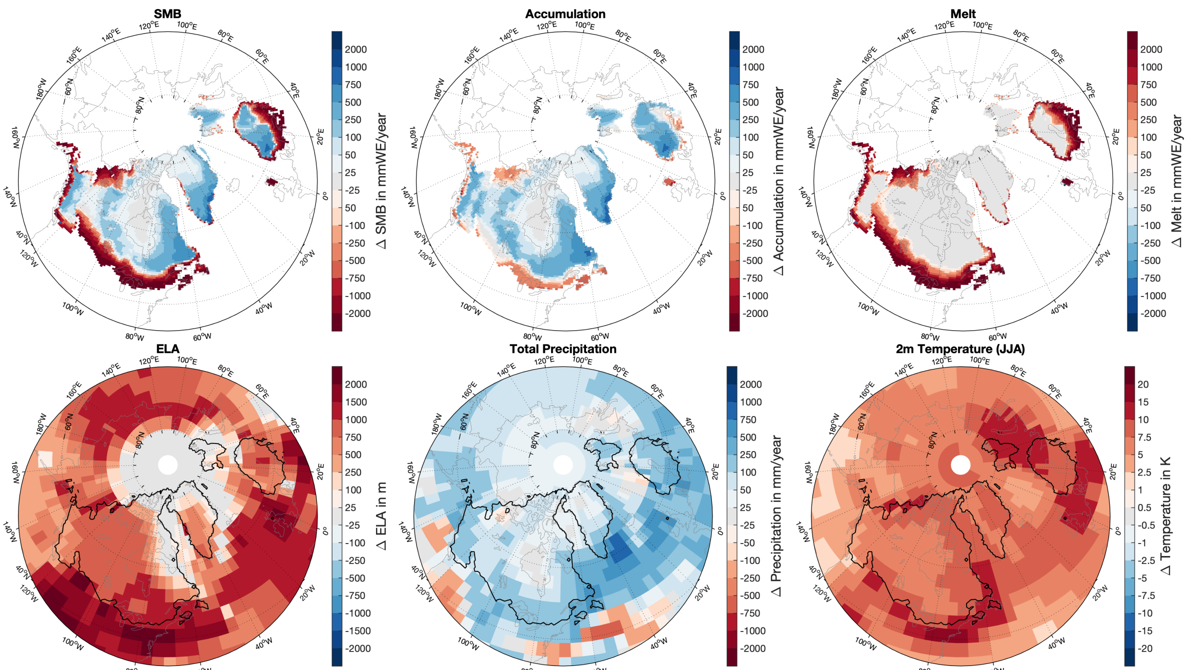

Figure 5. Differences of SMB, accumulation and melt, precipitation and 2-m temperatures as well as summer 2-m summer temperatures between 15 ka ~~BP~~ and the LGM. For the differences SMB, accumulation and melt are interpolated on the Glac1D topography of each individual time slice. The other variables are shown on the native MPI-ESM-CR model grid. Black contours in the lower panels indicate the ice-sheet mask at 15 ka~~BP~~.

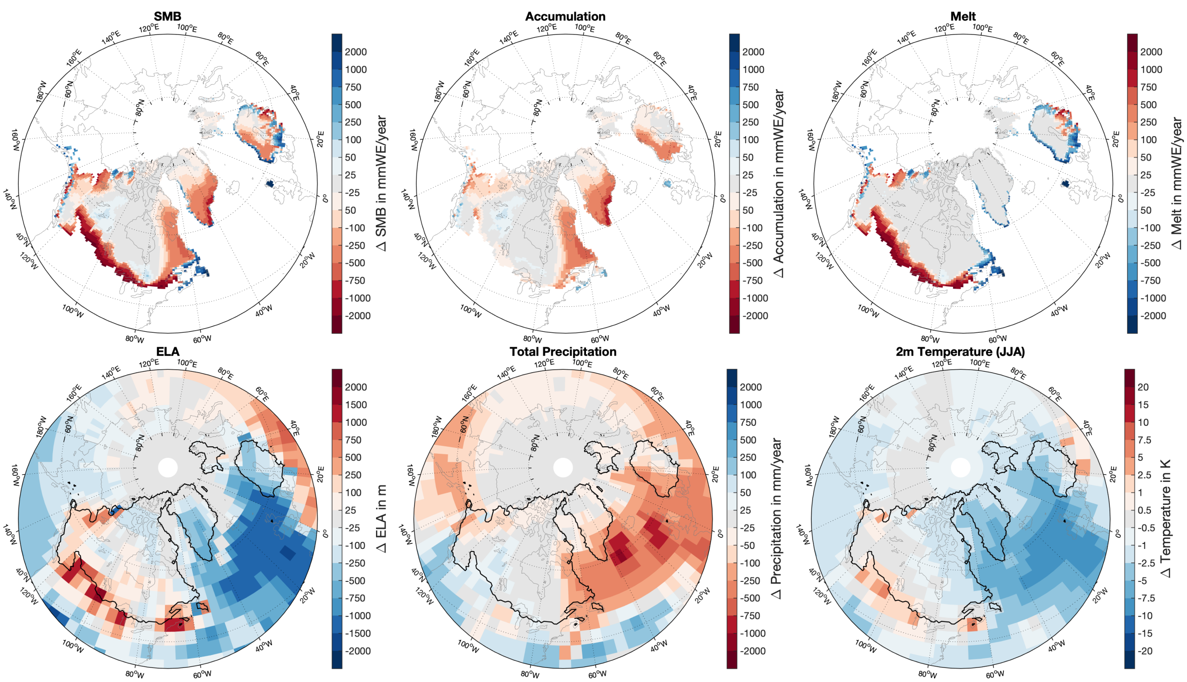

Figure 6. Similar to Fig. 5, but for differences between 14.6 ka and 15 ka~~BP~~.

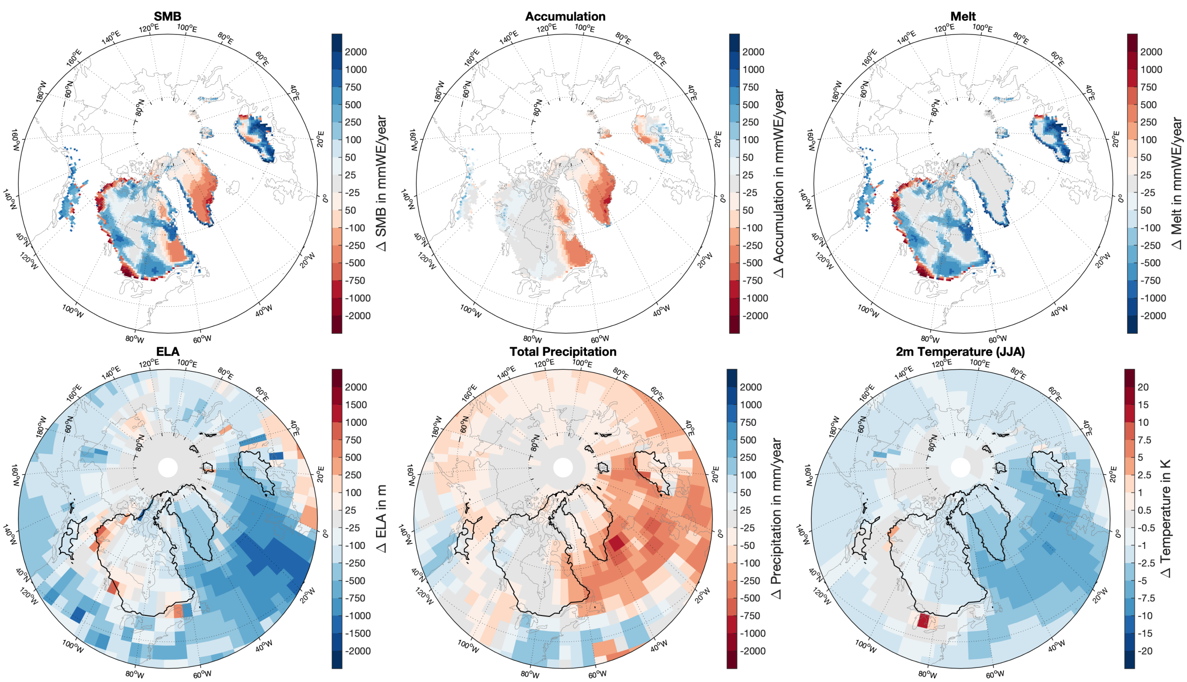

Figure 7. Similar to Fig. 5, but for differences between 11.6 ka and 12 ka~~BP~~.

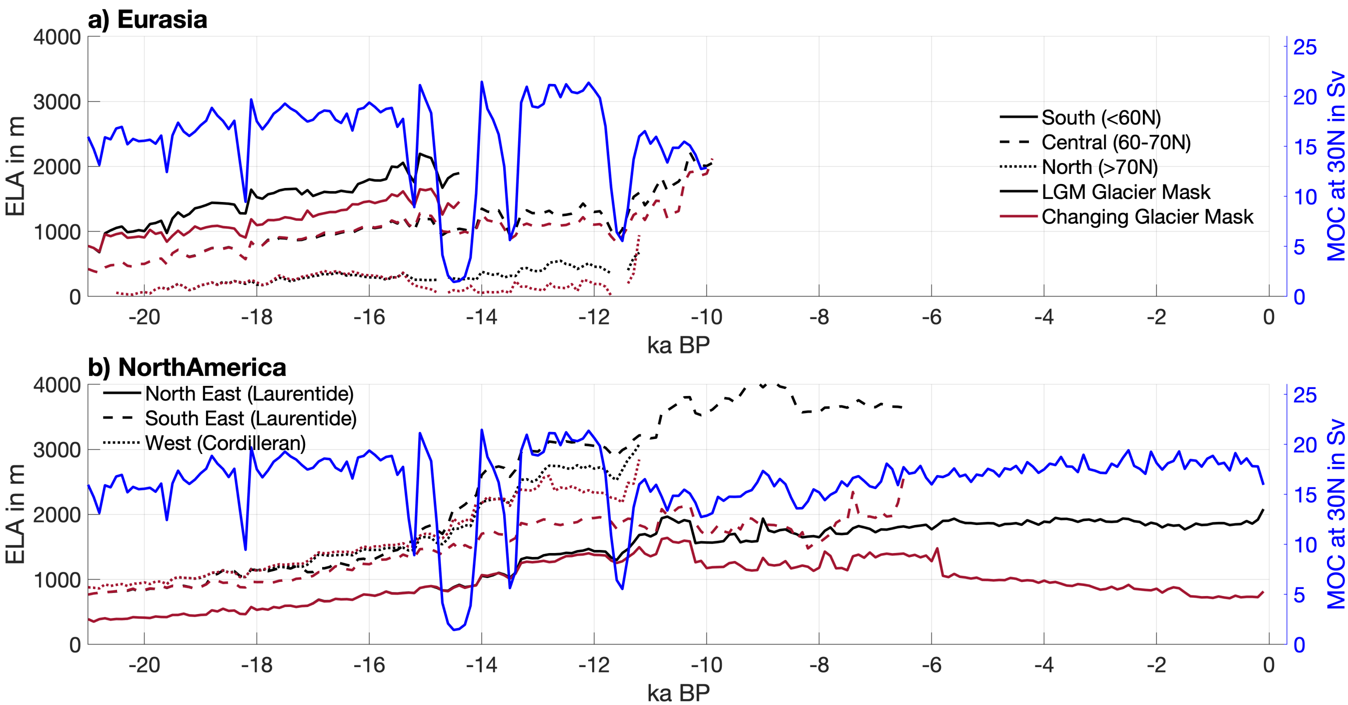

Figure 8. Similar to the bottom panel of Fig. 3 but for the sub-divided (a) Eurasian and (b) North American ice sheets. The Eurasian ice sheet is subdivided into a southern (<60°N), central (60°-70°N) and northern (>70°N) part. The North American ice sheet is split into the northern and southern Laurentide ice sheet (east of 120°W and north of 60°N and south of 60°N, respectively) and the Cordilleran ice sheet (west of 120°W). The ELA is integrated for each region over the 21 ka ~~BP ice sheet~~ ice-sheet mask (black) and over the ~~ice sheet~~ ice-sheet mask of each respective time slice (red).

Table 1. Elevation classes used in the EBM.

Elevation level	1	2	3	4	5	6	7	8	9	10	11	12
Height over sea level in m	0	100	200	300	400	500	625	750	875	1000	1125	1250
Elevation level	13	14	15	16	17	18	19	20	21	22	23	24
Height over sea level in m	1375	1500	1625	1750	1875	2000	2500	3000	4000	5000	6000	8000

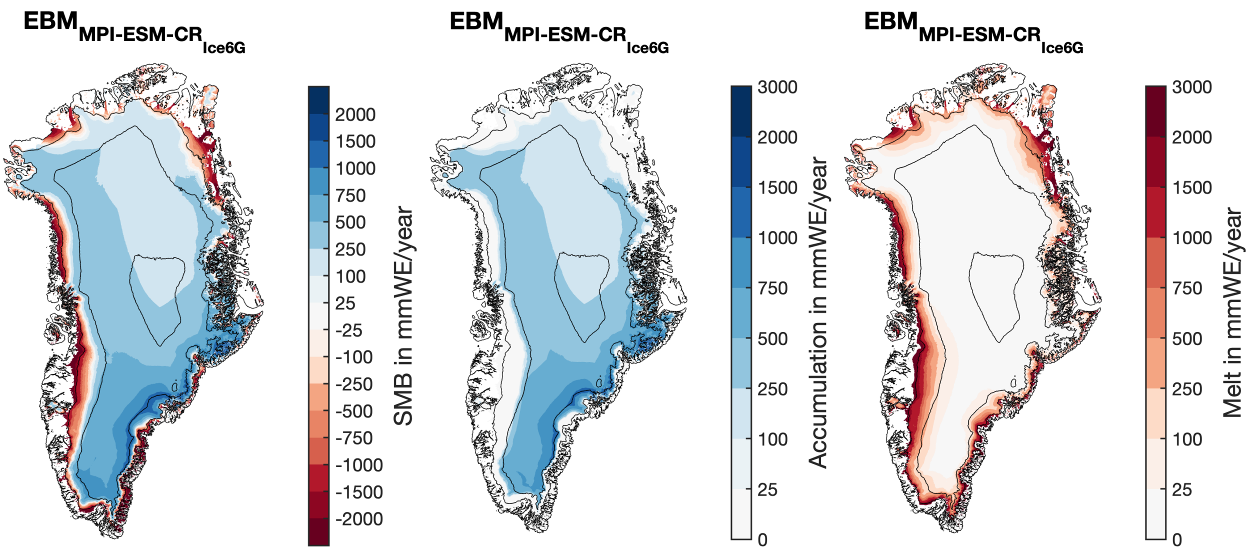

Figure A1. Similar to Fig. 1 but for the MPI-ESM-CR$_{\text{Ice6G}}$ simulation.

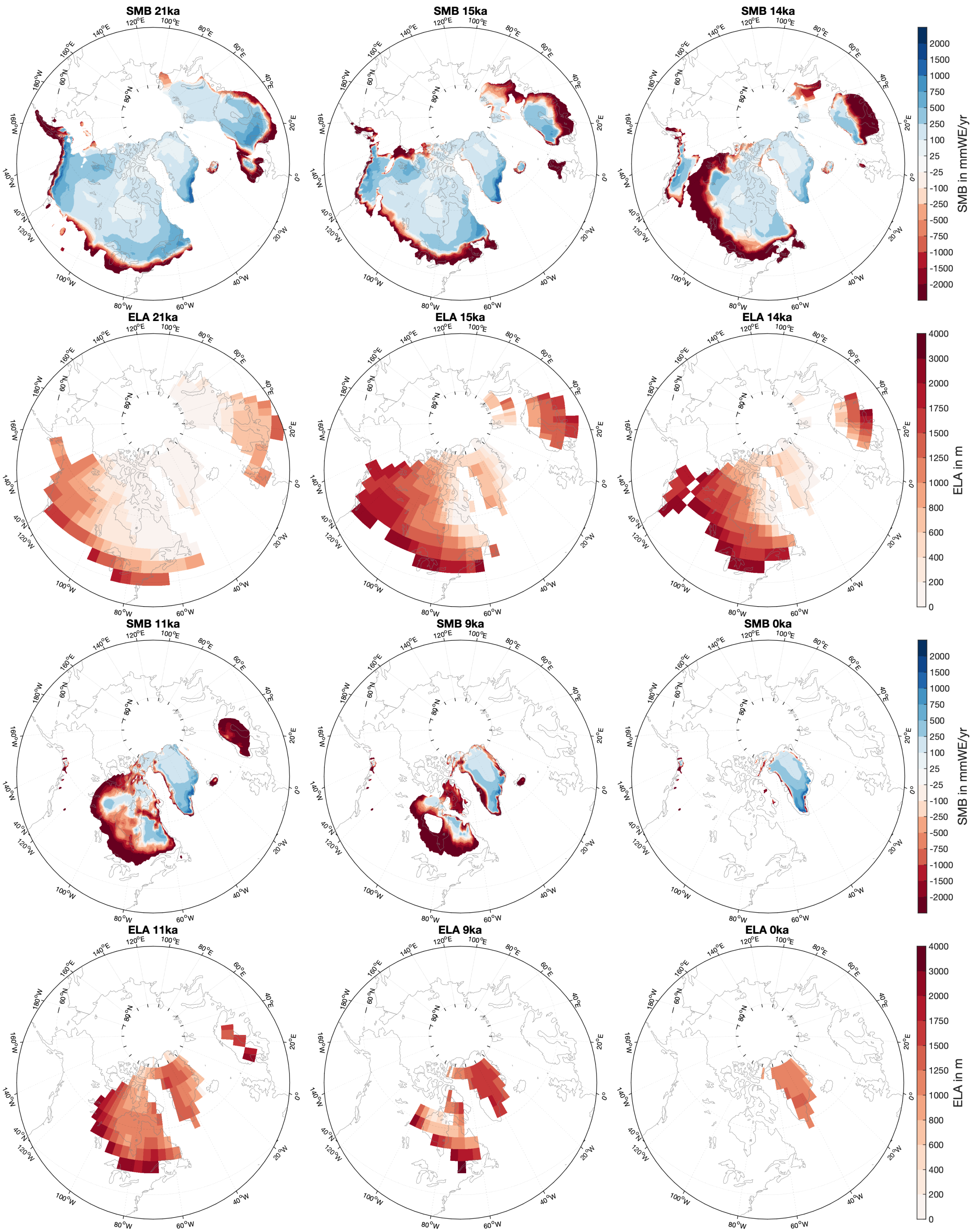

Figure A2. SMB and ELA for selected time slices (21 ka, 15 ka, 14 ka, 11 ka, 9 ka and 0 ka~~BP~~). Shown are 100-year means. The SMB is interpolated on the ICE-6G topography for each individual time slice, the ELA is shown on the native MPI-ESM-CR model grid. Note that the different glacier masks are a result of the different resolution

.

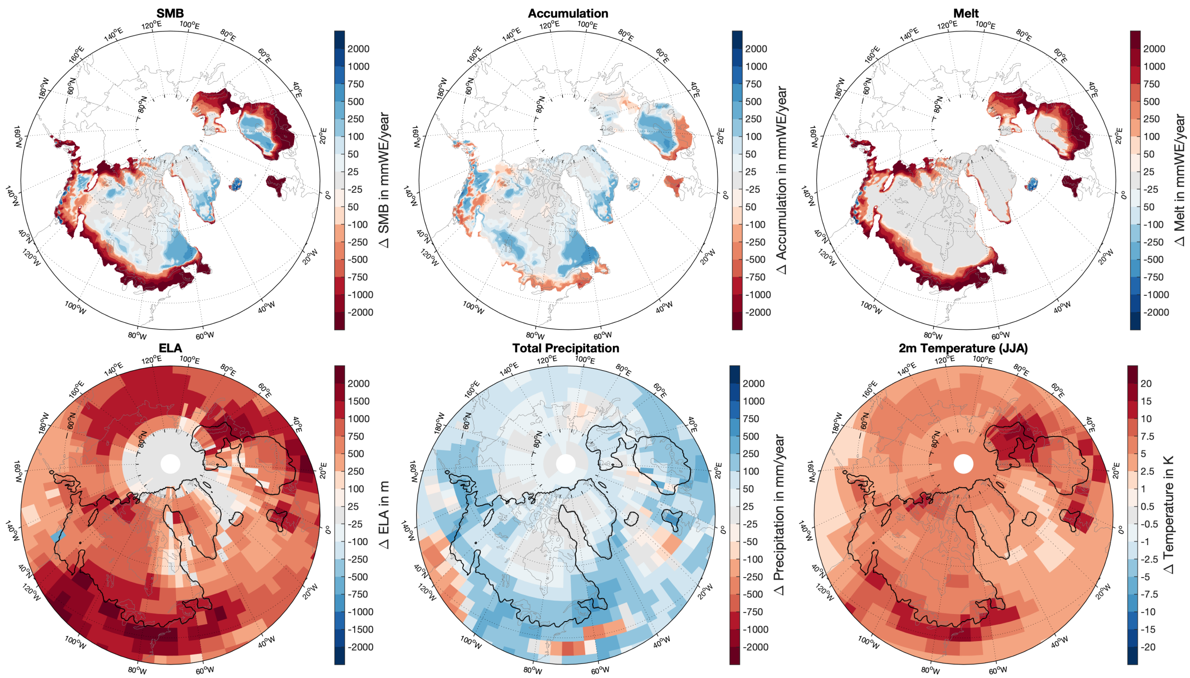

Figure A3. Similar to Fig. 5 but for differences between 15 ka and LGM from MPI-ESM-CR$_{\mathrm{Ice6G}}$.

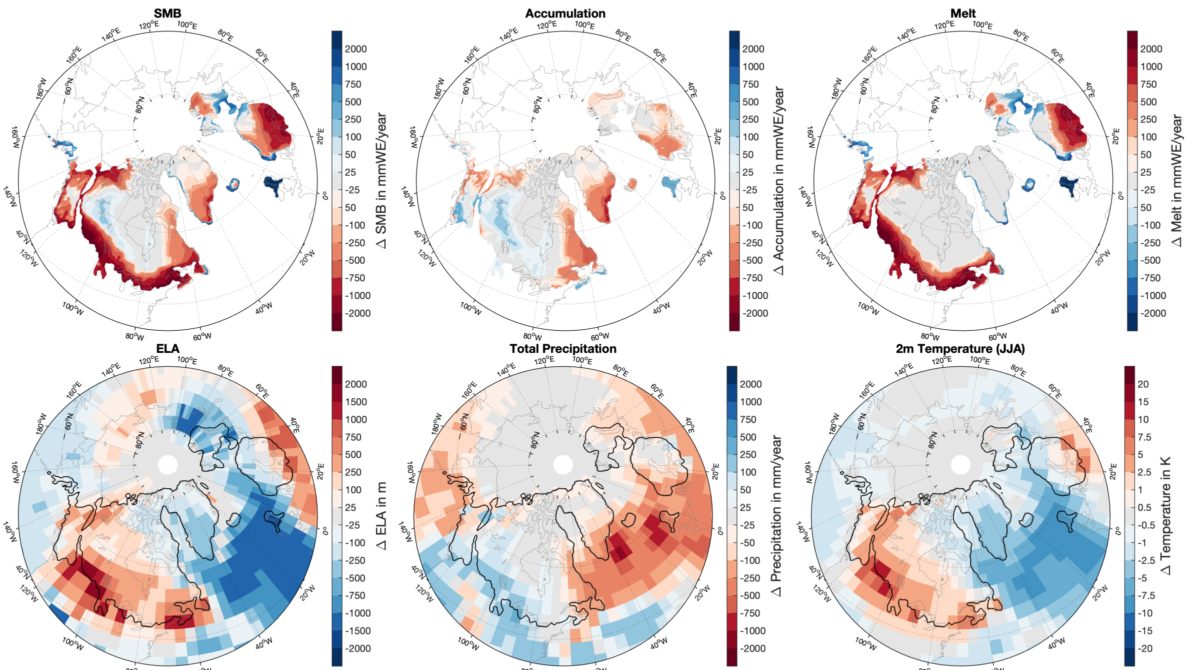

Figure A4. Similar to Fig. A3, but for differences between 14.4 ka and 15 ka ~~BP~~ from MPI-ESM-CR$_{\mathrm{Ice6G}}$. Note, that a different time slice was chosen as compared to Fig. 6 due to a later AMOC slowdown in the MPI-ESM-CR simulation with Ice-6G boundary conditions.

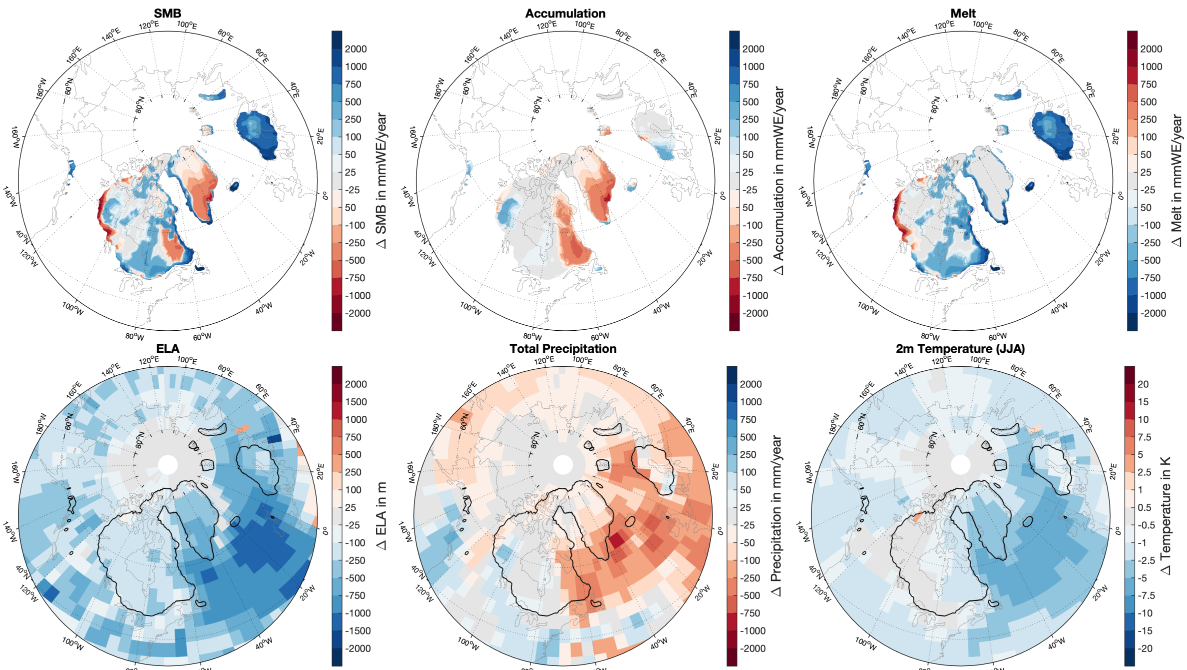

Figure A5. Similar to Fig. A3, but for differences between 11.2 ka and 12.2 ka ~~BP~~ from MPI-ESM-CR$_{\mathrm{Ice6G}}$. Note, that a different time slice was chosen as compared to Fig. 7 due to different timings of the AMOC slowdown in MPI-ESM-CR with Ice-6G boundary conditions.

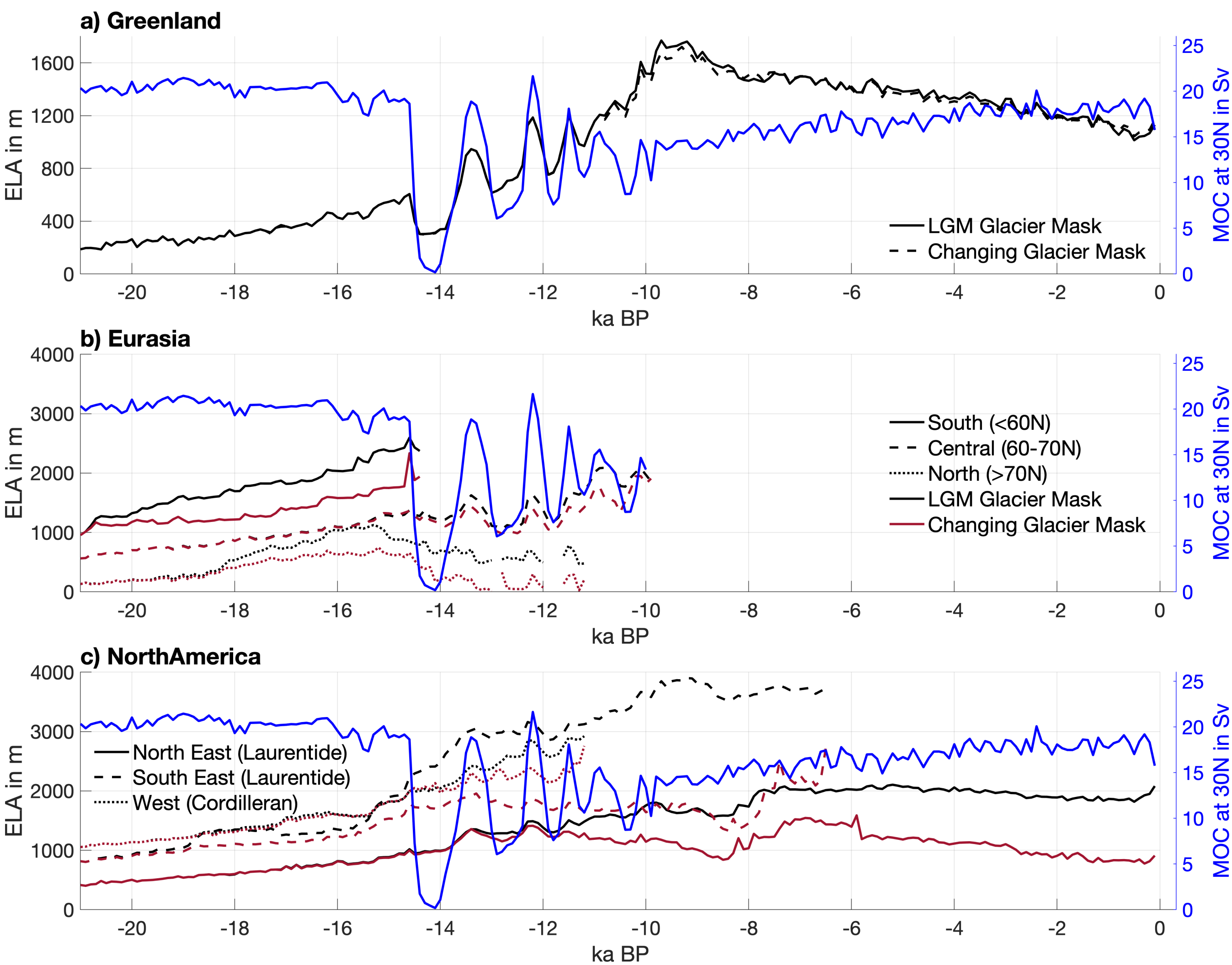

Figure A6. Similar to Fig. 3 and 8 but for $\mathrm{EBM}_{\mathrm{MPI-ESM-CRIce6G}}$ with prescribed Ice6G reconstructions.